Functional analysis of Protocadherin18a in zebrafish early development

Zur Erlangung des akademischen Grades eines

DOKTORS DER NATURWISSENSCHAFTEN

(Dr. rer. nat.)

der KIT-Fakultät für Chemie und Biowissenschaften

des Karlsruher Instituts für Technologie (KIT)

genehmigte

DISSERTATION

von

Bernadett Bősze

aus Mosonmagyaróvár, Ungarn

KIT-Dekan: Prof. Dr. Willem Klopper

Referent: Dr. Steffen Scholpp

Korreferent: Prof. Dr. Martin Bastmeyer

Korreferent: PD Dr. Dietmar Gradl

Tag der mündlichen Prüfung: 16. 12. 2016

Gedruckt bzw. veröffentlicht mit Unterstützung des Deutschen Akademischen Austauschdienstes

Erklärung

hiermit erkläre ich, dass ich die beigefügte Dissertation selbstständig verfasst und keine anderen als die angegebenen Hilfsmittel genutzt habe. Die aus fremden Quellen direkt oder indirekt übernommenen Gedanken sind als solche gekennzeichnet. Des Weiteren habe ich die Satzung der Universität Karlsruhe (TH) zur Sicherung guter wissenschaftlicher Praxis in der jeweils gültigen Fassung beachtet. Die elektronische Version stimmt mit der schriftlichen überein. Die Abgabe und Archivierung der Primärdaten gemäß. Abs. A (6) der Regeln zur Sicherung guter wissenschaftlicher Praxis des KIT ist beim Institut gesichert. Diese Arbeit wurde bisher weder in gleicher noch in ähnlicher Form einer anderen Prüfungsbehörde vorgelegt, nicht veröffentlicht und, dass diesem Promotionsverfahren keine endgültig gescheiterten Promotionsverfahren vorausgegangen sind.

Publications

Gross J. C., **Bösze B.**, Scholpp S. and Boutros M.
Wnt3A induces cancer cell migration via autocrine Wnt5A secretion (Manuscript in preparation)

Bösze B., Sinner C., Stricker K., Gourain V., Thumberger T., Weber S., Wittbrodt J., Strähle U., Schug A. and Scholpp S.
Pcdh18a positive tips cells orchestrate notochord formation (Manuscript under review in Developmental Cell)

Acknowledgement

This thesis would not have been possible without the dedicated work of several individuals who in many ways contributed to the completion of this research project. I wish to acknowledge those who during these three years extended their valuable assistance in my PhD work.

My first debt of gratitude must go to my supervisor, Dr. Steffen Scholpp, who patiently provided advice and encouragement for me to progress on personal levels and to complete the doctoral program.

I would like to thank lab members, past and present, for their expert advice and for their invaluable help offered in developing my technical skills. I want to specially thank Sabrina and Benjamin for their great assistance to do this research. I would like to thank Kathrin Stricker, a motivated Bachelor student in our lab for her invaluable contribution to my project. My sincere thanks also go to all my colleagues and staff in the Institute of Toxicology and Genetics for their excellent support. I also want to thank DAAD for their financial support granted through a doctoral fellowship. I would also like to thank Pritesh Krishnakumar for the interesting and useful discussion on this project over the years. I also thank Shariq Ansari, who provided great support and assistance during the development of this project. I also want to acknowledge Dr. Thomas Dickmeis, who reviewed drafts of my thesis and provided valuable comment.

Last but not the least, I would like to thank my loving family who always supported me and encouraged me in every step of doing this work.

Contents

Figure index

Abbreviations

CE – convergence and extension

E-cad – E-cadherin

Fzd7a – Frizzled7a

Gsc - goosecoid

NTC – notochord tip cells

Ntl - notail

Pcdh18a – Protocadherin18a

Abstract

"It is not birth, marriage, or death, but gastrulation, which is truly the most important time in your life." (Lewis Wolpert, 1986).

Gastrulation is a pivotal phase of early embryonic development and leads to the formation of the defining axial structure of all Chordates: the notochord. It is essentially the result of major cell rearrangements and is driven by the coordinated movement of mesodermal cells, often referred to as collective cell migration. Cohesion is guided by various factors and stays connected via cadherin-based junctions. In recent years, significant interest has been focused on the largest group within the cadherins superfamily, the protocadherins. The presence of protocadherins in the nervous system has commanded the most attention while little is known about their role in cell-cell adhesions in early development.

In this work, I defined the role of Pcdh18a, a novel member of protocadherins in zebrafish gastrulation. Pcdh18a is expressed in a confined cell group – termed the notochord tip cells and exhibit strong connection to the trailing notochord progenitors. At the molecular level, Pcdh18a mediates the recycling of E-cadherin and thereby affects the migratory capabilities of cells. Using the Cellular Potts model, we were able to simulate the migration of mesodermal cells in early zebrafish development. Our model predicted that high motility and strong adhesiveness of Pcdh18a-positive prechordal plate is a prerequisite of proper axis formation during gastrulation.

1 Introduction

1.1 Zebrafish as a model in developmental biology

The basic developmental mechanisms across the animal kingdom are well conserved and evolutionary related proteins play an important role in establishing the body pattern and specifying cell types in the developing embryo.

Developmental biology depends on the use of animal models to understand the organization of an embryo on cellular and molecular levels. Due to the striking homology across mammalian genomes, systems such as mice and rats have been utilized to model human development as well as to create disease models that recapitulate the pathology of human disorders. On the other hand, conserved cellular mechanisms underlying human disease have been accurately modeled at genetic and molecular levels in the worm Caenorabditis elegans and in the fruit fly Drosophila melanogaster.

Since the pioneering work of George Streisinger in the 1970's, the teleost zebrafish (*Danio rerio*) has emerged as a fantastic alternative to mammalian and invertebrate species, particularly in studying the genetic control of embryonic development. This is due to the fact that zebrafish combine a number of unique and ideal features for developmental biologists. Its development and the different developmental stages have been well described (Kimmel et al., 1995) and are explained in detail in the Appendix (Figure 31).

Zebrafish are easy to maintain and breed all year with a large clutch of embryos; an adult female can lay up to 300 eggs a week. The embryos develop *ex utero* - outside the mother, which makes them easily accessible for genetic manipulations (microinjection, cell transplantation assays). Furthermore, the embryos are transparent which allow the easy visualization of morphological changes and cell movements *in vivo* as well the tracking of fluorescently labeled proteins in an intact environment.

Furthermore, the development of genetic techniques such as cloning, mutagenesis and transgenesis, strengthened the importance of zebrafish in addressing questions of vertebrate development. Its use in forward genetic screens has led to the identification of hundreds of developmental mutants (Brockerhoff et al., 1995) and further established zebrafish as an invaluable model in developmental biology.

1.2 Embryonic development

1.2.1 General introduction

In the course of embryogenesis, through successive mitotic divisions and finely tuned and controlled processes, a single cell generates the complex three-dimensional structure of a multicellular organism. Although embryogenesis is a continuous process, it is generally categorized into different stages that highlight particular events. For example, during cleavage, a series of cell divisions occur in the fertilized egg generating the so-called blastomeres. In the process of gastrulation, the blastomeres undergo major cell rearrangements and generate the primary germ layers – ectoderm, mesoderm and endoderm and the major axes of the embryo are determined. Following gastrulation, the cells interact to generate the primary tissues and organs of the body. The end of embryogenesis is characterized by the hatching or birth of the embryo. In many species, the organism further undergoes metamorphosis to reach a sexually mature state. Despite the incredible diversity of animal species, these characteristics of embryonic development are shared across the animal kingdom.

Nevertheless, gastrulation is often referred to as the key stage in embryonic development. Its importance has been emphasized in the famous phrase by Lewis Wolpert: “It is not birth, marriage or death, but gastrulation, which is truly the most important time in your life.” (Wolpert, 1986). Gastrulation is indeed a complex process that entails a vast array of coordinated cell behaviors, including for example the dynamic rearrangements of cells. Cellular movements occurring during gastrulation are evolutionary conserved and involve internalization and spreading of cells and the convergence and extension of the tissue. These morphogenetic movements are essential to the proper positioning of cells within the embryo and define the final outcome and shape of the developing organism. Therefore, it is fundamental to understand the cellular and molecular mechanisms that underlie the complexity of gastrulation.

1.2.2 Morphogenetic movements in gastrulation

Gastrulation is a fundamental morphogenetic process in embryogenesis during which the germ layers – ectoderm, endoderm, and mesoderm - are formed and specified. It is

defined by dramatic cellular rearrangements within the embryonic body. These cell movements comprise three major features: epiboly, internalization and convergent extension of cells (Keller, 1991).

Epiboly starts before the specification of the germ layers and is associated with the spreading and thinning of the superficial layer of the embryo. Epiboly can be achieved by different mechanisms within vertebrates (Figure 1 a). For example, in fish and frogs, epiboly is driven by the upwards movements of blastomeres – a process called radial intercalation which ultimately leads to the thinning of the tissue (Keller, 1980, Warga and Kimmel, 1990). In higher vertebrates such as amniotes, epiboly is achieved by the constant division and expansion of cells within the plane of the epithelium (Solnica-Krezel and Sepich, 2012).

The entire process of internalization can be described as the detachment of cells from the epithelium – characterized by epithelial-to-mesenchymal-transition (EMT) and their subsequent movement as prospective mesodermal and endodermal cells into the inside of the embryo (Solnica-Krezel and Sepich, 2012). In zebrafish, cells internalize at the side of the embryonic margin, the equivalent structure in frogs is called the blastopore lip and the primitive streak in amniotes. Different modes of internalization can be distinguished among species (Figure 1 b). During Drosophila gastrulation, presumptive mesoderm cells invaginate at the ventral midline of the embryo and subsequently break their connections in the epithelium and migrate to the inside of the embryo. In frog gastrulation, precursor cells involute at the site of the blastopore lip and move as a cohesive sheet. In amniotes, presumptive mesodermal cells first detach from the epithelium and translocate as individuals to deeper positions in the embryo, in a process called ingression. In zebrafish, a combination of ingression and involution occur. Cells internalize at the embryonic margin as individuals (ingression), however in a synchronized manner that resembles the involution of cells that accompanies internalization in frogs.

The third major morphogenetic movement during gastrulation is the narrowing (convergence) and lengthening (extension) of the embryonic axis commonly referred to as convergence extension (CE) (Figure 1 c). CE movements have been best studied during Xenopus gastrulation (Keller et al., 1985). Here the narrowing and elongation of the embryonic axis occurs via the medio-lateral (ML) intercalation of cells. Cells become polarized along their ML axis and intercalate with their neighbours. In frogs, medio-lateral intercalation is the sole way of forming an elongated axis. Similarly in

mouse, cell intercalation plays an important role in the formation of the axial mesoderm. In zebrafish, two modes of convergence and extension movements occur: cells can migrate actively in a collective fashion (collective migration) or cells can acquire ML polarity and intercalate in the midline. In chick gastrulation, convergence extension is driven by the regression of the primitive streak (Tada and Heisenberg, 2012).

Different species employ similar strategies although with different variations to generate the elongated shape of the embryo and establish the body plan by the end of gastrulation.

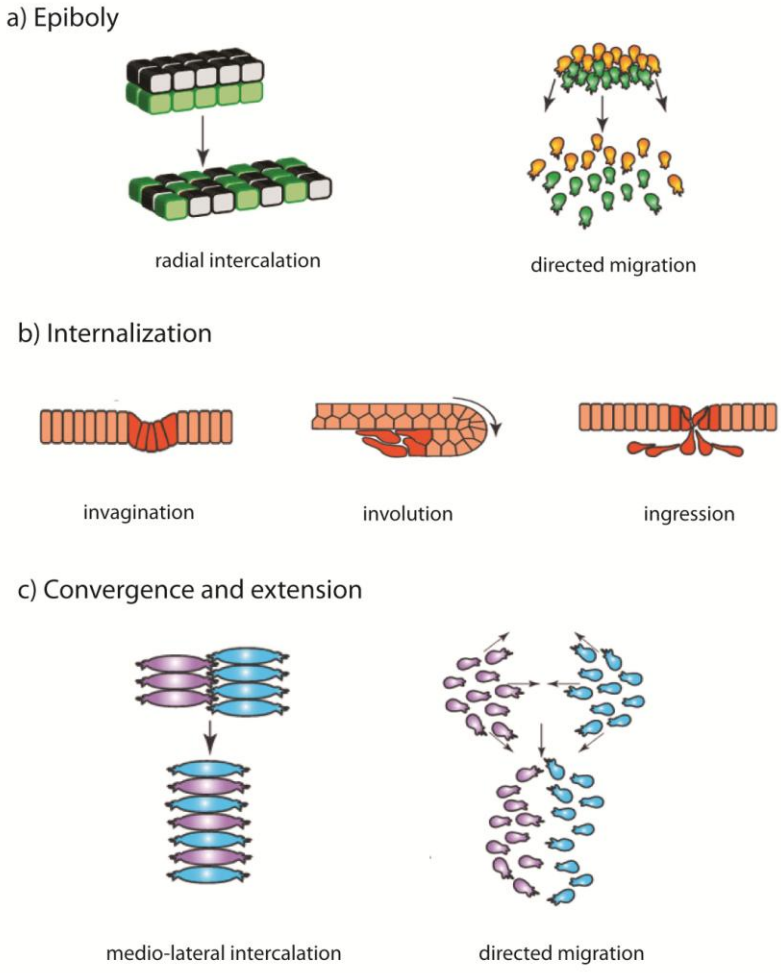

Figure 1 Different types of morphogenetic movements during gastrulation

The three main features of morphogenetic movements: Epiboly (a) that can be accomplished by either the movement of cells within the thickness of the tissue or by directed movements of single cells. Internalization modes (b) can also differ among species, invagination of cells is a typical principle in Drosophila, involution occurs in frogs and single cell ingression is characteristic to amniote embryos. Convergence extension movements can be driven by the medio-lateral intercalation of cells (c) or by the collective and directed migration of cell groups. Adapted from (Solnica-Krezel and Sepich, 2012)

1.2.3 Gastrulation in zebrafish

Gastrulation in zebrafish has been extensively studied and involves a combination of cellular movements that make the entire process of gastrulation a highly complex event. After the initial cleavage stages, the blastomeres are formed atop of the yolk and morphogenetic movements become evident and continue throughout gastrulation, shaping and reorganizing the embryonic body (Figure 2).

Epiboly starts as early as 5 hours after fertilization; the blastoderm starts to spread over the yolk cells and by the end of gastrulation it completely engulfs the yolk (Warga and Kimmel, 1990). At 50% epiboly, the blastoderm covers half of the yolk and cells start to accumulate at the embryonic margin, forming a thickening called the germ ring (Warga and Kimmel, 1990). Cells simultaneously start to internalize dorsally and then throughout the entire margin. By that time, the blastoderm constitute of a superficial layer called epiblast and the underlying hypoblast, the progenitor of endoderm and mesoderm. At the beginning of internalization, cells move individually, via ingression movements (Carmany-Rampey and Schier, 2001). As gastrulation proceeds, mesodermal progenitor cells move as a cohort towards the animal pole.

Convergent extension (CE) movements start simultaneously with cell internalization. At 50% epiboly, a local thickening of cells at the dorsal margin marks the onset of convergent extension. This compaction forms the embryonic shield, the zebrafish equivalent of the Spemann organizer that is essential to the proper formation of the embryonic body axes (Warga and Nusslein-volhard, 1998). Cells deriving from the embryonic shield form the axial structures in the midline: the anteriormost prechordal plate, followed by the precursor of the notochord, the chordamesoderm (Trinkaus, 1992). Cell internalizing at the lateral margin give rise to the somites and the lateral plate (Kimmel et al., 1990). The ventralmost mesodermal cells do not migrate dorsally and contribute to the formation of the tailbud at the end of gastrulation(Myers et al., 2002) (von der Hardt et al., 2007).

Cell behaviors driving gastrulation movements have been best studied in the frog Xenopus leavis (Elul and Keller, 2000). Gastrulation is triggered by the involution of mesendodermal progenitors and their movements are entirely driven by medio-lateral cell intercalation, leading to the narrowing and lengthening of the forming embryonic axis. However, in zebrafish a similar morphogenetic outcome can be reached by a different variety of cell behaviors. Cell movements in the zebrafish lateral plate are

under the control of convergence movements, the prechordal plate cells undergo active migration towards the animal pole, while the organization of notochord largely depends on the intercalation of axial mesodermal progenitors (Friedl and Gilmour, 2009). Migratory defects in the lateral plate mesoderm have only little effect on the intercalation of the notochord progenitors, while defects in cell intercalation usually result in impaired body axis elongation (Bakkers et al., 2004, Heisenberg et al., 2000) (Glickman et al., 2003, Sepich et al., 2000). The prechordal plate cells exhibit active migration that takes place in a highly coordinated fashion (Heisenberg, Tada et al. 2000). Interfering with the integrity of the prechordal plate progenitors leads to the uncoordinated migration of prechordal plate cells (Ulrich et al., 2005). Therefore in zebrafish, a variety of movements exist; intercalation of notochordal progenitors, the convergence of lateral plate mesoderm cells and the active and collective migration of prechordal plate cells, all of which are essential for body axis elongation.

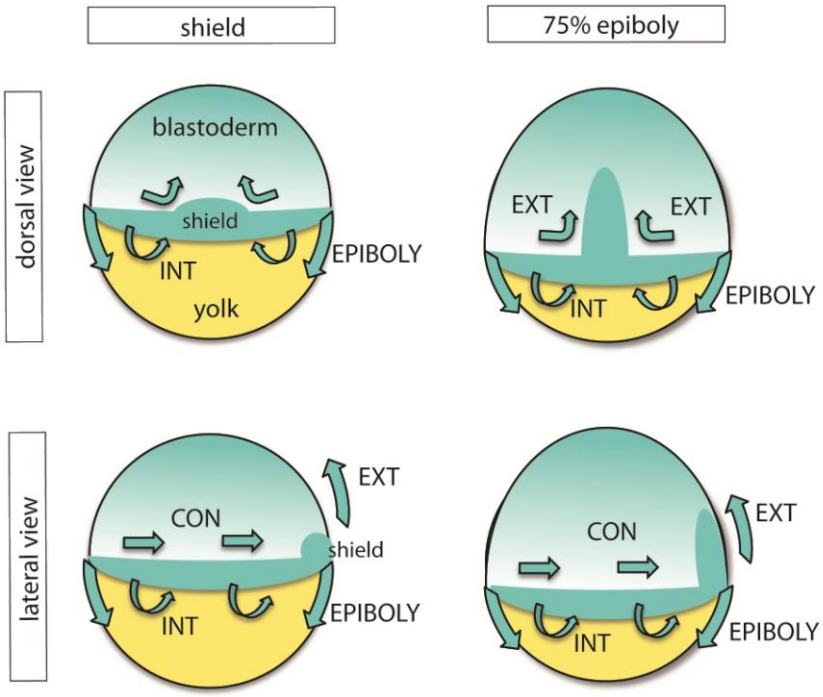

Figure 2 Principle cell movements during zebrafish gastrulation.

The onset of gastrulation is marked by the formation of the shield, however morphogenetic movements by epiboly start already at late blastula stages. As gastrulation progresses, cells internalize at the embryonic margin, most dominantly at the side of the shield and start migrating towards the animal pole. Simultaneously, cells converge towards the midline and extend along the antero-posterior axis.
INT –internalization, CON – convergence, EXT – extension

1.3 Molecular mechanisms of cell rearrangements during gastrulation

To understand the variety of morphogenetic movements, one first needs to explore the underlying mechanisms on the cellular and molecular level, which has been a challenging task. Gastrulation entails a combination of cellular movements, which require the translocation of cells from one position to another. First, cells need to change their behavior and gain migratory properties in order to migrate. To do so, cells change their shape, become polarized, alter their adhesive capabilities and employ different signaling pathways that keep cell behavior under control.

1.3.1 Cell migration

Cell motility plays an essential role in biological processes. For instance, during gastrulation, coordinated and directed movement of cells shape and reorganize the embryonic body. During epithelial-to-mesenchymal transition (EMT), cells downregulate epithelial characteristics, lose their contacts and polarity and acquire a mesenchymal phenotype that facilitates their migration (Nieto, 2011). Cell motility is also one of the hallmarks of tissue repair and wound healing, the ability of organisms to protect themselves against injuries. Cell migration further contributes to tissue renewal and regeneration. For example, in the renewal of the small intestine, epithelial cells migrate upwards from the Lieberkühn crypts onto the surface of the villi (Crosnier et al., 2006). Migration is also essential in immunosurveillance in which immune cells migrate into tissues looking for pathogens and destroying invading microorganisms. Nevertheless, cell migration has been implicated as a prominent factor in pathological conditions such as cancer metastasis. It leads to the invasion of cancerous cells, and it also contributes to various diseases such as osteoporosis and vascular disease.

Two basic principles of cell migration exist. Cells can migrate as individuals; in this case no stable cell-cell contacts are established and the cells move in a rather uncoordinated way towards their destination (Friedl and Gilmour, 2009). For instance, single immune cells circulate the blood and pass through a tissue which is an essential function for immunosurvaillence. Interestingly, the infiltration of tumor cells into the adjacent tissues can also be achieved by their individual migration. Examples of

single cell migration in zebrafish include the migration of primordial germ cells into the gonad (Reichman-Fried et al., 2004) and to some extent, the individual movement of the internalizing mesendodermal progenitors (ingression) at the onset of gastrulation (Rohde and Heisenberg, 2007).

However, a more common way of cell migration involves the directed movement of cells in a highly organized and coordinated fashion. During collective migration, cell stay connected to their neighbors and the migration of the cell group is governed by the interaction of individual cells. It is important to distinguish collective migration from the movement of cells triggered by chemotaxis, in which the overall cell movement of a group is triggered by external cues (Friedl and Gilmour, 2009).

Collective cell migration contributes to various aspects of development in different species (Scarpa and Mayor, 2016). For example, the branching of tubular structures such as the trachea or blood vessels requires the collective migration of cells. The lateral line, the mechanosensory organ of the fish is also assembled by the cohort migration of cells. Collective migration of cells also characterizes many aspects of vertebrate gastrulation. In frogs, mesodermal progenitors internalize as a cohesive group (invagination) in contrast to amniotes in which cells internalize individually (ingression). In zebrafish, cells internalize individually but migrate towards the anterior of the embryo as a cohort. Last but not least, collective migration plays a prevalent role in pathological conditions such as the collective invasion of cells in cancer metastasis.

Directed cell movement is one of the hallmarks of gastrulation. However, besides collective cell migration, cell intercalation is another important way of organizing tissues. Cell rearrangements and the subsequent elongation of the body axis are mostly driven by cell intercalation. During radial cell intercalation, cell exchange neighbours throughout the thickness of the tissue and is one of the driving factors of gastrulation and epiboly movements. Radial intercalation also occurs during skin development and in the thinning of the ventral mesoderm in Drosophila (Walck-Shannon and Hardin, 2014).

In medio-lateral intercalation cells exchange positions in the same plane and it is the driving factor of convergence and extension during gastrulation. Medio-lateral intercalation is not only important for axis elongation during gastrulation, but it also contributes to the elongation of the trachea in Drosophila and elongation of the kidney in vertebrates (Scarpa and Mayor, 2016).

Although a vast array of migration modes exists, the underlying mechanisms all require cytoskeletal rearrangements, cell polarization, modulation of cell-cell connectivity by adhesion molecules and guidance by signaling molecules.

1.3.2 Cytoskeletal rearrangements and force generation

In order for cells to change their position, they first need to establish polarity and induce rearrangements of the actin cytoskeleton (reviewed in (Mayor and Etienne-Manneville, 2016). When polarity is established, the cell can be divided into a leading edge and a trailing edge. In the leading edge, activation of small GTPases such as Rac1 and CDC42 drive the polymerization of the actin cytoskeleton, which results in the formation of membrane protrusion such as lamellipodia and filopodia. Cell protrusions on the leading edge sense the environment and drive the directed movement of the cell. On the other hand, the posterior edge of the cell (trailing edge) is characterized by dynamic retractions. Although these are the basic principles of cell polarity establishment in single cells, the same mechanism can be applied to collectively migrating cell groups. However, when cells migrate as a cohort, individual cells acquire different roles relative to their position within the group. This means that cells at the front edge of the migrating group called leader cells are able to sense their microenvironment – a property called mechanosensing and follow guiding cues in order to direct the migration of the entire cell group. Cells located in the core of the group or at the posterior edge are called follower cells. As the name suggests, they follow instructions given by the leader population. But what exactly are these instructions and how are they followed?

During migration, at the front edge of the cell, not only membrane protrusions are formed by the activation of cytoskeletal rearrangements but also cell traction forces are generated by the polymerization of actin filaments (Mayor and Etienne-Manneville, 2016). Traction is however not well balanced over the entire cell, which results in a net force, pushing the cell in a particular direction. This also means that the front edge of the cell exerts forces that are sufficient to pull and coordinate the migration of the entire cell. How are these forces transmitted within a group of cells? In a migrating cohort, leader cells generate most of the traction and pull the followers with them. Leader cells sense their environment through mechanosensing, which

includes various proteins and their conformational changes, in particular cell-cell adhesion molecules that mediate the attachment of cells to each other or to their environment. Traction forces generated by the leader cells are also transmitted via adhesive structures and the actomyosin network. Similarly to leader cells, followers also exhibit mechanosensing properties, which allow sensing their environment, including information transmitted from the leaders.

In a migrating cohort, cell-cell connections are essential in order to keep the cell together and for the transmission of information. Cell-cell connections are established by cell-cell adhesion protein; the most prominent members belong to the superfamily of cadherins. Protrusive activity and cell traction is affected in embryos mutant for cadherins and ultimately this results in defects of cell migration during gastrulation (Hong and Brewster, 2006) (Montero et al., 2005).

1.3.3 Cell adhesion molecules

The organization of tissues into organs is determined by molecular interactions at the cell surface and requires the precisely regulated temporal and spatial expression of a wide array of adhesive molecules (Cavallaro and Dejana, 2011). Cells can adhere indirectly through the binding of adhesion receptors to components of the surrounding extracellular matrix (ECM). Cells also adhere directly to one another through specialized integral membrane proteins called cell-adhesion molecules (CAMs) that often cluster into specialized cell junctions.

The primary CAMs in adherens junctions belong to the cadherin family. Cadherins were originally identified three decades ago as calcium dependent glycoproteins (hence their name calcium adhering) that mediate homophilic interactions between neighboring cells (Yoshida and Takeichi, 1982) and modulate cell-cell adhesion via dynamic interactions with the cytoskeleton. The cadherin family can be divided into categories according to their structural and functional properties: classic cadherins (types I and II and desmosomal cadherins), and a large group of atypical cadherins which includes the flamingo, FAT, and protocadherin (pcdh) families (Halbleib and Nelson, 2006) (Figure 3).

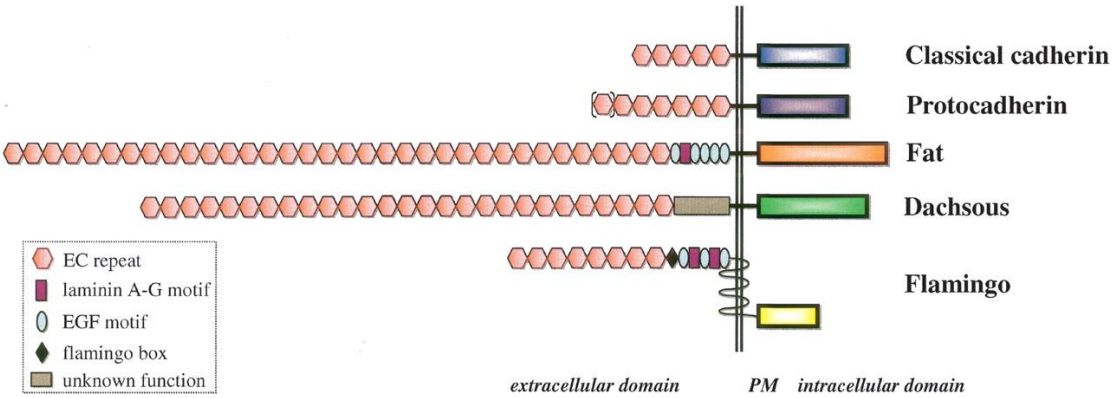

Figure 3 Classification in the cadherin superfamily

Cadherins can be categorized based on their domain characteristics. Classical cadherin contain five Ca^{2+} binding domain in the extracellular domain, and via their intracellular domain they are connected to the actin cytoskeleton. Protocadherins contain six or seven Ca^{2+} domain and their cytoplasmic domain is variable, showing no connection to actin filaments. Atypical cadherins such as Fat, Dachsous and Flamingo carry multiple cadherin domains and various cytoplasmic tails (Halbleib and Nelson, 2006)

Classical cadherins

Classical cadherins are key proteins in cell-cell adhesion and cell signaling. On a structural level, they contain a single transmembrane domain, a C-terminal cytosolic domain and five extracellular cadherin domains. The extracellular domain is necessary for Ca^{2+} binding and cadherin-mediated cell-cell adhesion. The C-terminal intracellular domain is highly conserved and linked to the actin cytoskeleton by adapter proteins such as catenins. This connection is essential for strong cell-cell adhesion. The intracellular domain of cadherins can interact with other cytoplasmic proteins such as β-catenin and p120-catenin; β-catenin mediates cytoskeletal attachment, which has an important role during traction force generation and polarity establishment. P120-catenin might act as a regulator of cadherin stability at the cell surface (Jenkins et al., 2013).

Different subtypes of classical cadherin were described in distinct tissues: for example, E-cadherin in epithelial cells, N-cadherin in the nervous system and P-cadherin in placenta cells (Takeichi, 1988). However, their distribution is not limited to the tissue from which they were first isolated and cadherin switching within a tissue is a physiologically prevalent event and occurs already during gastrulation. The conversion from E-cadherin to N-cadherin is observed during neurulation and in the

process of epithelial-to-mesenchymal transition. Switches in cadherin expression have been also implicated in tumor progression (Paul et al., 1997).

Classical cadherin also have an essential role during cell movements in gastrulation. When E-cadherin-mediated cell-cell adhesion is disrupted, epiboly movements are perturbed (Shimizu et al., 2005). In zebrafish, E-cadherin (e-cad) is expressed maternally in all blastomeres. As gastrulation progresses, *e-cad* is expressed in the anterior axial mesoderm and has been shown to mediate cell adhesion during gastrulation movements, although the precise mechanism is unknown (Babbs et al, 2001).

Protocadherins

In the past decade, function of protocadherins has been extensively studied in various model systems. With over 70 members, protocadherins (pcdhs) represent the largest group within the cadherin superfamily (Sano et al., 1993).

They generally contain six or seven extracellular cadherin repeats, a single transmembrane domain or multiple domains (Fat- and Dachsous-related), and diverse cytoplasmic regions that do not interact directly with β-catenin as classical cadherins do (Yoshida et al., 1999).

Based on their chromosomal arrangements, protocadherins can be categorized into subfamilies: clustered protocadherins (α, β, and γ-family) and non-clustered protocadherins (δ-family) (Hirano et al., 2003) (Aoki et al., 2003).

The δ-pcdhs can be further subdivided into two subgroups, δ1 and δ2, based on the number of extracellular cadherin repeats (seven versus six), and conservation of the cytoplasmic domains (Redies et al., 2005). The δ1 subgroup comprises Pcdh1, -7, -9, and -11; the δ2 subgroup comprises Pcdh8, -10, -17, -18, and -19.

Many members of the δ-family have been reported to facilitate weak cell–cell adhesion in vitro (Sano et al., 1993) (Hirano et al., 1999) or to influence the proper gastrulation of vertebrate embryos (Kim et al., 1998).

In Xenopus gastrulation, mesodermal progenitor cells sort out based on their protocadherin expression and specifically label the axial (AXPC) or the paraxial (PAPC) mesoderm (Kim et al., 1998). PAPC also affects adhesion by regulating the activity of C-cadherin (Chen and Gumbiner, 2006).

Mouse Pcdh18, another δ2-pcdh, interacts with Disabled-1 (Homayouni et al., 2001) a protein involved in the Reelin pathway and needed for correct formation of cortical neuron layers (Howell et al., 2000). Although Pcdh18 was described in mice, not much is known about its role in embryonic development (Figure 4). It has been suggested that during zebrafish gastrulation, Pcdh18a can affect morphogenetic movements, although the exact mechanism needs to be elucidated (Aamar and Dawid, 2008).

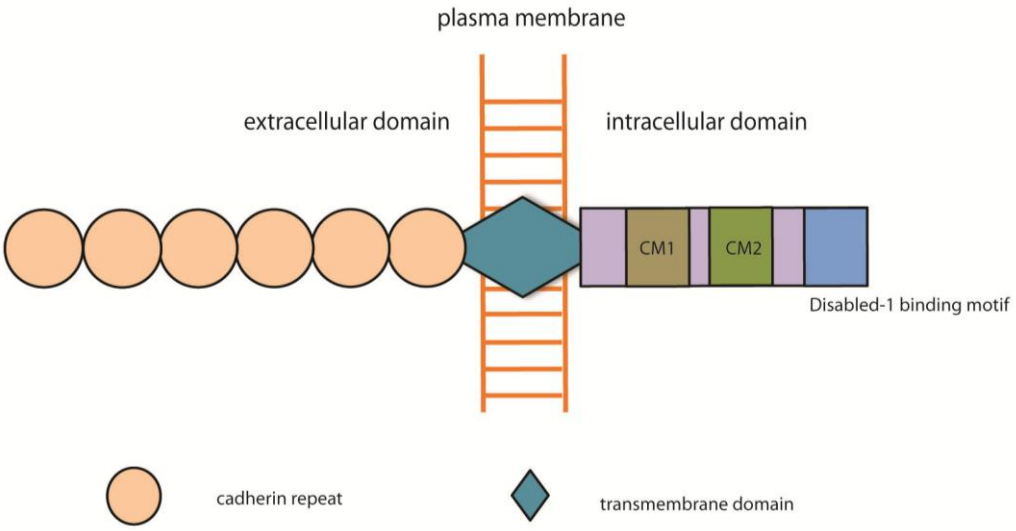

Figure 4 Structure of Pcdh18a in zebrafish

Pcdh18a protein shows a structure typical for protocadherins. The extracellular domain contains six Cadherin repeats that are able to bind Ca^{2+} ions. The protein has a single transmembrane domain (TM). In the intracellular domain, it carries two conserved domains (CM1 and CM2) and a Disabled-1 binding motif.

1.3.4 Controlling surface proteins

In the course of development, the amount or nature of cell-surface cadherins changes, affecting many aspects of cell-cell adhesion and cell migration. Fibroblasts expressing different type of cadherins sort out in a mixed cell population and different levels of the same cadherin during germ layer formation are important for the sorting out of cells (Duguay et al., 2003) (Steinberg, 2007). For instance, the reorganization of tissues during morphogenesis is often accompanied by the conversion of epithelial cells into motile mesenchymal cells. These processes are associated with the reduction in the expression of E-cadherin. Furthermore, conversion of epithelial cells into

cancerous melanoma cells is also marked by the loss of E-cadherin activity. This decrease in cell-cell adhesion permits melanoma cells to invade the underlying tissue and spread throughout the body. Therefore, dynamic and controlled regulation of cadherin concentrations at cell surfaces is a major way of determining cell behavior. But what are the molecular mechanisms that underlie changes in cadherin expression at the cell surface?

Cadherin levels can be first controlled on the transcriptional level. This kind of modification has been implicated in cancer progression. Methylation of the E-cadherin promoter reduces transcription of the gene and leads to reduced E-cadherin level which ultimately results in tumor progression (Thiery, 2002) (Strathdee, 2002).

Cell adhesion can be directly mediated at the cell surface by ADAM metalloporeasesor presenilin and the release of cadherin domains could disrupt adhesion (Baki et al., 2001). Cadherin stability can also be controlled by p120-catenin binding partner as loss of p120 results in endocytosis of E-cad (Jenkins et al., 2013).

However, the most common strategy for cells to control signaling activity and proteins at the cell surface is endocytosis. For example, endocytosis of E-cad in clathrin-coated vesicles can result in rapid loss of adhesion (Fujita et al., 2002). During endocytosis, membrane proteins and their binding partners are brought into the cell by budding of plasma membrane vesicles. After internalization, proteins can be transported back to the membrane, in a process called recycling or they can be targeted for degradation by their delivery to the lysosomal pathway.

Endocytic vesicles can be typically distinguished based on the Rab proteins they carry in their membrane. Rab proteins belong to the family of small GTPases and serve as the master regulators of vesicular membrane transport. Rab5 is associated with the early endocytic pathway (Roberts et al., 2000); Rab7 is localized to late endosomes (Chavrier et al., 1990); and Rab11 regulates recycling of endocytosed proteins (Takahashi et al., 2012). The lysosomal membrane protein LAMP1 is predominantly found in the lysosomes (Cook et al., 2004).

The importance of recycling has been demonstrated in various developmental processes. For example, during tracheal branching in Drosophila, cells form the tubular structure of the trachea by intercalation. It has been shown that higher levels of E-cad due to recycling makes the decision to inhibit intercalation, while lower levels allow intercalation (Scarpa and Mayor, 2016).

The dynamic physiological regulation of the adhesive functions of cadherins at the cell surface is especially important for many morphogenetic processes, such as cell sorting, cell rearrangements and cell movements.

Protocadherins similarly seem to be affected by trafficking machinery. γ-protocadherins are present largely in intracellular organelles, and with low levels in the cell membrane (Murata et al., 2004). The control of their trafficking appears to rely in the cytoplasmic domain as deletion of the domain result in increase surface delivery (Schreiner and Weiner, 2010).

Interestingly, the regulated endocytosis and recycling of cadherins are under the control of the PCP signaling pathway and necessary for example the proper establishment of polarity within the Drosophila wing (Devenport, 2014).

1.3.5 Wnt/PCP signaling pathway

Planar cell polarity (PCP) refers to the polarized orientation of cells within the plane of a tissue (Devenport, 2014). The evolutionary conserved mechanism of planar cell polarity was first described in Drosophila and has been extensively investigated ever since (Mlodzik, 1999, Seifert and Mlodzik, 2007).

The core pathway components include the transmembrane receptors of the Frizzled family which recruit Dishevelled (Dvl) to the distal side of the cell. On the opposite cell surface, other antagonistic transmembrane proteins (Strabismus/VanGogh) accumulate and interact with Prickle (Solnica-Krezel and Sepich, 2012). Such asymmetric distribution of proteins establishes the cell polarity; also in entire tissues for example in the eye ommatidia (Adler, 2002).

In vertebrates, the PCP homologous signaling pathway includes additional members of the non-canonical Wnt family. The Wnt family of glycoproteins consists of secreted signaling molecules that upon binding to their Frizzled receptor can trigger downstream effectors and lead to changes in cell behavior such as cell movement, cell polarity and cell proliferation (Gray et al., 2011) (Figure 5).

Wnt/PCP pathway is the major signaling pathway during gastrulation, affecting different aspects of the morphogenetic movements. For example, in the prechordal plate, the anterior migration of cells in dependent on wnt11; in mutant embryos (*silberblick*), migratory behavior of cells is perturbed, cell protrusions are randomized which overall influences the directed movement of cells (Ulrich et al, 2003).

Furthermore, the dorsal migration of cells is impaired in *trilobite*/*knypek* double mutants (Strabismus and Glypican mutants, respectively), the cells are less polarized and exhibit a roundish shape.

Wnt/PCP signaling is also necessary for the convergent extension movements in zebrafish and Xenopus (Heisenberg et al., 2000; (Wallingford et al., 2002). The cytoskeleton is one of the targets of non-canonical Wnt signaling (Veeman et al., 2003) indicated by the defective orientation of actin-rich protrusions in PCP mutants (Ulrich et al., 2003). Non-canonical Wnt has been also shown to modulate cell adhesion (Solnica-Krezel, 2006). Defects of cell adhesion were also observed in response to loss of Fzd7 function in Xenopus (Winklbauer et al., 2001).

In zebrafish, mutants of the Wnt/PCP pathway have been primarily identified on the basis of the broad and short body axis at the end of gastrulation that indicates impaired cell behaviour during gastrulation ((Hammerschmidt et al., 1996); Heisenberg et al., 2000). Therefore, Wnt/PCP signaling in vertebrates is a crucial pathway for the coordination of global spatial cues with cell movement and orientation to achieve appropriate tissue morphogenesis.

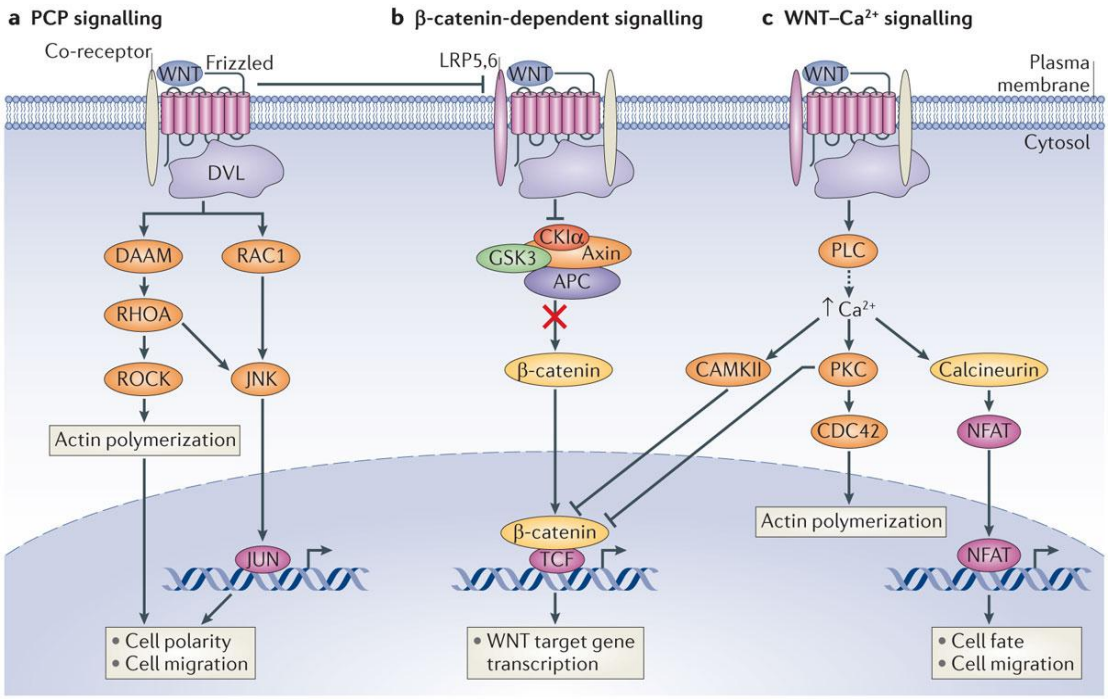

Figure 5 Branches of the Wnt signaling family

During signaling, Wnt ligands bind to their receptor at the cell surface, which triggers the signaling cascade. The canonical pathway depends on β-catenin activity and binding of the Wnt ligands results in the accumulation of β-catenin in the cytoplasm and its subsequent translocation to the nucleus where in interaction with TCF/LEF transcription factors it mediates target gene function. In the non-canonical branches Wnt/PCP and Wnt/Ca^{2+}, the pathway is independent of β-catenin function and signaling results in cytoskeletal rearrangements and cell-cell adhesion changes. Adapted from (Niehrs, 2012)

1.3.6 Other signaling pathways in gastrulation

Besides the Wnt pathway, other signaling cascades are at play during gastrulation. Nodal related genes (*cyclops* and *squint*) control tissue morphogenesis and are required for the formation of the embryonic shield (Feldman et al, 1998, 2000). Consequently, inactivation of Nodal antagonist genes (*lefty*) results in the expansion of the mesoendoderm and failure in epiboly movements (Feldman et al., 2002). This indicates that Nodal signals are required and sufficient to induce both mesendodermal cell fate and the morphogenetic cell behaviors underlying mesendodermal cell internalization during vertebrate gastrulation.

PDGF/PI3K (Platelet Derived Growth Factor/Phosphoinositide-3-kinase) signaling is important for cell polarization and subsequent migration during gastrulation (Symes and Mercola, 1996). JAK/STAT signaling also functions as a regulator of cell

movements, by controlling cell adhesion and cytoskeletal rearrangements through Rac1 (Simon et al., 2000).

Signaling through Stat3 (Signal Transducer and Activator of Transcription 3) is also essential in the dorsal regions of the gastrula for the activation of the anterior migration of cells (Yamashita, 2002). Interestingly, BMP signaling also plays a pivotal role during morphogenetic movements. It has been shown that mesodermal cells require BMP signals in order to speed up convergence towards the midline BMP negatively regulates cell-cell adhesion and creates a gradient of cell adhesiveness from the ventral to the dorsal regions of the embryo. This gradient is essential for determining the directionality of migration (Myers, 2002).

Aims of this study

Recent studies have identified Protocadherin18 as a diverse protein, being involved in a variety of processes throughout development. It has been implicated to play a role in the correct formation of cortical neuron layers in mouse (Homayouni et al., 2001), it has been shown to be an inhibitor of T-cell receptor signaling in tumors (Vazquez-Cintron et al., 2012) and in humans, it can be linked to intellectual disabilities (Kasnauskiene et al., 2012).

In zebrafish, however, little is known about its importance. The purpose of this work was to characterize a novel member of the cadherin superfamily (Protocadherin18a – Pcdh18a) and identify its function in early zebrafish development. Pcdh18a has been reported to affect epiboly and cell movements during gastrulation (Aamar and Dawid, 2008). However the molecular mechanism how Pcdh18a could facilitate cell motility in gastrulation or whether it affects cell-cell adhesion has not been investigated. It is therefore important to uncover the mechanism by which Pcdh18a can enhance membrane motility at cell–cell interfaces, and how these processes promote cell migration and contribute to the proper establishment of the vertebrate body plan.

2 Material and Methods

2.1 Materials

2.1.1 Equipment and tools

NAME	DESCRIPTION
Absorbance reader	Microtiterplate reader (VERSAmax)
Dissection forceps	Fine Tip No. 5 (Dumont)
Glass needle	1.0mm outer ⌀, 0.58 mm inner ⌀, with filament (TW100,WPI Inc.)
Microinjector	Femtojet with integrated pressure supply (Eppendorf)
Microloader tips	930001007 (Eppendorf)
Micromanipulator	Manual, M3301R (WPI Inc.)
Microscopes	Olympus SZX10/SZX16 Leica SP5 TCS confocal microscope Leica SP2 two photon confocal microscope Leica DMI6000 SD Zeiss Axiovert 200M
Needle holder	Microelectrode holder (WPI Inc.)
Needle puller	P-97 Flaming/Brown Micropipette Puller (Sutter Instrument)
Odyssey imager Protein detector	Licor
Omnifix-F 0.01-1ml syringe	Braun, Melungen AG, Germany
PCR machine	GeneAmp PCR system 9700 (AB)
Photometer	Nanodrop (Thermo Scientific Inc.)
Rotilabo-syringe filters 0.22 um	Carl Roth GmbH, Karlsruhe
Tungsten needle	TGW1510, ⌀ 0.38mm (WPI Inc.)
Western blot systems	BioRad

2.1.2 Chemicals

NAME	COMPANY
Acrylamide	Carl Roth, Karlsruhe
agarose	Peqlab, Erlangen
Ampicillin	Carl Roth, Karlsruhe
Anti-digoxigenin Fab fragments	Roche, Mannheim
APS ammoniumperoxisulfat	Carl Roth, Karlsruhe
β-mercaptoethanol	Carl Roth, Karlsruhe
Bacto-agar	Carl Roth, KArlsruhe
BCIP	Roche, Mannheim
Blocking reagent for nucleic acids	Roche, Mannheim
Bovine Serum albumin (BSA)	PAA, Coelbe
Calcium acetate	Carl Roth, Karlsruhe
Calcium chloride	Sigma-Aldrich, Taufkirchen
Chloroform	Sigma-Aldrich, Taufkirchen
Citric acid	Carl Roth, Karlsruhe
Dimethylsulfoxide (DMSO)	Fluka, Neu-Ulm
Dithiothreitol	Carl Roth, Karlsruhe
Dulbecco's modified Eagle's medium (DMEM)	Invitrogen, Karlsruhe
Ethanol	Carl Roth, Karlsruhe
Ethidium bromide	Carl Roth, Karlsruhe
EDTA	Carl Roth, Karlsruhe
Fast red tablets	Roche, Mannheim
Fetal bovine serum (FBS)	BIOCHROM AG, Berlin
Formamide	Carl Roth, Karlsruhe
Glucose	Carl Roth, Karlsruhe
Glycerol	Carl Roth, Karlsruhe
Glycine	Carl Roth, Karlsruhe
Heparin	Carl Roth, Karlsruhe
HEPES	Carl Roth, Karlsruhe
Hydrochloric acid	Merck, Darmstadt

Isopropanol	Carl Roth, Karlsruhe
Kalium chloride	Sigma-Aldrich, Taufkirchen
Kanamycin	Sigma-Aldrich, Taufkirchen
Leibovitz's L-15 medium	Gibco, Karlsruhe
Low-melting agarose	Carl Roth, Karlsruhe
Methanol	Carl Roth, Karlsruhe
Mini-Emerald	Thermo Scientific, Darmstadt
NBT/BCIP stock solution	Carl Roth, Karlsruhe
NP-40	Carl Roth, Karlsruhe
Paraformaldehyde	Merck, Darmstadt
Penicillin/Streptomycin	Invitrogen, Karlsruhe
PBS	Invitrogen, Karlsruhe
Pronase	Carl Roth, Karlsruhe
Proteinase K	Sigma-Aldrich, Taufkirchen
Sodium acetate	Carl Roth, Karlsruhe
Sodiumdodecylsulphate (SDS)	Carl Roth, Karlsruhe
Sodium chloride	Carl Roth, Karlsruhe
TEMED	Carl Roth, Karlsruhe
Tris base	Carl Roth, Karlsruhe
Tris HCL	Carl Roth, Karlsruhe
Triton-X 100	Carl Roth, Karlsruhe
Trypsin 0.25% -EDTA	Invitrogen, Karlsruhe
Tween 20	Carl Roth, Karlsruhe
Yeast extract	Carl Roth, Karlsruhe

2.1.3 Softwares

NAME	**COMPANY**
Cell-A	Olympus, Rodgau
ImageJ/Fiji	NIH
Imaris	Bitplane AG, Zurich
Las AF	Leica, Wetzlar

2.1.4 Enzymes

NAME	COMPANY
Cas9 nuclease	Thermo Fisher Scientific
DNase I	Ambion, Kaufungen
Fast Digest Eco31l	Thermo Fisher Scientific
Pfu DNA polymerase	Promega Mannheim
Restriction enzymes	New England Biolabs, Ipswich
Reverse Transcriptase	Promega, Mannheim
Sp6 RNA polymerase	Life Technologies, Darmstadt
T7 RNA polymerase	Life Technologies, Darmstadt
Taq polymerase	Promega, Mannheim

2.1.5 Antibodies

NAME	COMPANY
Anti-DIG	Roche Diagnostics, Mannheim
Anti-FITC	Roche Diagnostics, Mannheim
Anti-GFP	Sigma, Darmstadt
Anti-mCherry	Sigma, Darmstadt
Anti-Pcdh18a	Sigma, Darmstadt
IR Dye 700	Li-cor, Bad Homburg
IWR 800 CW	Li-cor, Bad Homburg

2.1.6 Molecular biology kits

NAME	COMPANY
DIG/FITC RNA Labelling	Roche Diagnostics, Mannheim
Illustra ProbeQuant G-50 Microcolumns	GE Healthcare Europe
PeqLAb Gel Extraction Kit	VWR, Darmstadt
Pierce BCA Protein Assay	Thermo Fisher Scietific, Darmstadt

Plasmid Midi Kit	Qiagen, Hilden
SuperScript® III RT synthesis	Invitrogen, Darmstadt
mMachine Messenger Kit (Sp6, T7)	Ambion, Kaufungen

2.1.7 Culture media and agar plates

LB (Luria Broth)-media:

0.5% Yeast extract (Gibco BRL)

200mM NaCl

1 % Trypton (Difco)

to 1000ml with H2O

autoclaved, stored at 4°C

LB (Luria Broth)-plates:

2% Agar (Gibco) in 1 L LB-medium,

autoclaved, cool down to 40°C,

add 100mg/mL Ampicillin/Kanamycin, pour 20ml into Petri dishes and store at 4°C

2.1.8 Media for breeding and manipulation of zebrafish

1x Embryo rearing medium (E3):

0.1% NaCl

0.003% KCl

0.004% CaCl2 x 2H2O

0.016% MgSO4 x 7H2O

0.0001% methylene blue

1x MESAB:

400 mg tricaine powder (SIGMA)

2.1 ml 1 M TRIS (pH 9.0)

to 100 ml with H2O

adjust to pH 7.0 and store at 4°C

PTU:

0.003% 1-phenyl-2-thiourea in 1x PBS

2.1.9 Solutions in whole mount *in situ* hybridization

Stock solutions of 1 L were made.

MAB (5x):

58,04g maleic acid

43,83g NaCl

38g NAOH pellets

pH 7.5

MABT:

1x MAB + 0.1% Tween20

HYB^+ :

500 mL Formamide

250 mL 20x SSC (pH 6)

0.1% Tween20

0.5 mg/ml torula (yeast) RNA

50µg/ml Heparin

HYB^- :

500 mL Formamide

250 mL 20x SSC (pH 6)

0.1% Tween20

SSC (20x):

175,3g NaCl

88,2g Na_3Citrate

pH 6.0

SSCT:

1 x SSC + 0.1% Tween20

PBST:

1 x PBS + 0.1% Tween20

2.2 Methods

2.2.1 In vivo methods

Zebrafish husbandry

Adult zebrafish (*Danio rerio*) were maintained at 28.5 °C on a 14 h light/10 h dark cycle (Brand et al, 2002). The data in this research were acquired from the analysis of wild-type zebrafish (AB) and transgenic zebrafish lines:
tg(*-1.8 gsc:GFP*)$^{ml1(Dumortier\ et\ al.,\ 2012)}$ (Dumortier et al., 2012),
tg(h2afx:EGFP:rab5c)^{mw5Tg},
tg(h2afx:EGFPrab7)^{mw7Tg}
tg(h2afx:EGFPrab11a)^{mw6Tg} (Clark et al., 2011).

To introduce mRNA and antisense Morpholino oligonucleotides into fertilized zebrafish eggs, adult male and female zebrafish were first set up in the late afternoon in mouse cages with separators. The next morning, the separator was removed and fish were allowed to mate. Embryos were collected after 20 mins using a tea strainer and transferred to Petri dishes containing E3 medium.

2.2.2 Microinjection of zebrafish embryos

Prior to injection, capillaries with an internal filament were pulled on a Flaming-Brown puller according to the following parameters:

Pull-heat (H) 253
Pull-force (P) 40
Pull-velocity (V) 70
Pull-duration (T) 35

Capillaries were backfilled using Eppendorf microloader tips and the capillary tips were broken using sharp forceps under the microscope. For injection, the FemtoJet Microinjector with foot trigger and a microcapillary holder (micromanipulator fixed on a magnetic holder device) were used together with an Olympus stereomicroscope.

Zebrafish embryos were microinjected at one-cell stage or at eight-cell stage for generating clones. For confocal analysis, embryos were released from their chorion using Pronase and kept on agarose plates. Injected embryos were incubated at 28.5°C until the desired stage, and imaged using confocal microscopy or fixed in 4% paraformaldehyde in PBS overnight at 4°C and processed for *in situ* hybridisation.

2.2.3 Functional analysis

Transient knockdown of gene expression was performed using Morpholino oligonucleotides (MO). Pcdh18a function was inhibited by injecting a 0.5 mM concentration of each Morpholino oligomer at the one-cell stage.
The following antisense oligomers were used (Aamar and Dawid, 2008):

NAME	**SEQUENCE**
Control MO	5'-CGAAGTCTACGTCGGAATGCAGG-3'
Pcdh18a UTR MO	5'-TCCGTCAGGCACTGCAAAAATATAC-3'
Pcdh18a ATG MO	5'-ACCCTTGCTAGTCTCCATGTTGGGC-3'

In parallel, I used the CRISPR/Cas9 system to target the Pcdh18a locus. CRISPR (Clustered Regularly Interspaced Short Palindromic Repeats)/Cas9 technology represents a significant improvement over morpholinos, reaching a new level of efficiency, and ease of use. The CRISPR/Cas9 system takes advantage of the prokaryotic adaptive immune response that uses Cas9 endonuclease, guided by short, non-coding RNAs (Hwang et al., 2013). Cas9 induced double-stranded breaks are repaired either via non-homologous end joining (NHEJ) or homologous recombination (HDR). To create gene disruptions, a 20 basepair-long single guide RNA (sgRNA) complementary to the genomic sequence and flanking the so-called PAM (Protospacer Adjacent Motif) is generated to direct the Cas9 nuclease to a specific genomic location. The repair is error prone, and thus insertions and deletions may results in the disruption of gene function.

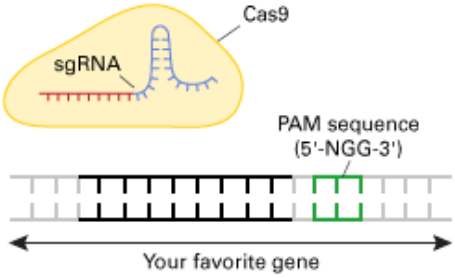

Figure 6 The concept of the CRISPR/Cas9 system.

The system requires two major components to be delivered in the organism: single guide RNA that is complementary to the target sequence in the gene of inetrest and flanked by the so-called PAM, a three-base-long motif that is essential for the efficient generation of double stranded breaks. sgRNA forms a complex with Cas9 protein and directs it to the site of action, where Cas9 cleaves the target DNA. DNA breaks are repaired by non-homologous-end-joining that is prone to error which can lead to the disfunction of the gene (modified after www.clontech.com).

All sgRNAs were designed and evaluated for potential off-target sites using CCTop, the CRISPR/Cas9 target online predictor (http://crispr.cos.uni-heidelberg.de/), selecting the target sequence 5' – CAGAGCAAGTTTGAGTAAAGTGG – 3'. For sgRNA assembly, a pair of synthesized oligomers was annealed, ligated into the DR274 (Addgene plasmid #42250) vector (Hwang et al., 2013), linearized with FastDigest Eco31l, and used for *in vitro* transcription with the T7 MegaShortScript Kit.

PLASMID NAME	SEQUENCE
Forward oligo	5' – TAGGGAGCAAGTTTGAGTAAAG – 3'
Reverse oligo	5' – AAACCTTTACTCAAACTTGCTC – 3'

Prior to injection, the Cas9 protein and sgRNA were diluted in RNAse-free water and incubated for 5 min at RT for complex formation (Burger et al, 2016).

For the overexpression studies, the following plasmids were used:

PLASMID NAME	SOURCE
Pcdh18a in pCS2^{+}	(Aamar and Dawid, 2008)

Pcdh18a-GFP in pCS2^{+}	(Aamar and Dawid, 2008)
Pcdh18a-mCherry in pCS2^{+}	Bernadett Bösze
Pcdh18aΔECD -mCherry in pCS2^{+}	Bernadett Bösze
Pcdh18aΔICD-mCherry in pCS2^{+}	Bernadett Bösze
GPI-anchored mCherry	Steffen Scholpp, KIT
GAP43-GFP	Steffen Scholpp, KIT
GPI-anchored mCFP	Steffen Scholpp, KIT
Histone-2-CFP	Steffen Scholpp, KIT
Frizzled7-CFP	Dietmar Gradl, KIT
E-cadherin-GFP	Erez Raz, University of Münster
E-cadherin-mCherry	Erez Raz, University of Münster

Capped and *in vitro* transcribed mRNAs (mMessage Machine Kit, Ambion) were microinjected into one-cell stage embryos.

2.2.4 Embryological manipulation assay

In transplantation set-ups, donor embryos were microinjected various constructs (see in Results) in combination with a lineage marker (mini-Emerald) at the one-cell stage. The host embryos were wild-type embryos. At the shield stage, 50 cells were removed from each donor embryo with a needle and injected into lateral mesoderm of the host embryos. The host embryos were then allowed to develop until 90% epiboly (9 hpf) and fixed for ISH.

In vivo two-photon laser-targeted ablation of individual cell rows in the axial mesoderm was performed with a Leica SP2. At one-cell stage, *gsc:GFP* embryos were injected with a red nucleus marker, and at 7hpf, were mounted with dorsal side up and ultrashort laser pulses were used to ablate the 5th GFP-positive cell row or the 15th GFP-positive cell row. The embryos were raised until 10 hpf for fluorescence imaging and subjected to ISH.

2.2.5 Compounds and inhibitors

Dechorionated embryos from the sphere stage to 80% epiboly were treated with 30 μM SB505124 (Sigma) to block mesoderm formation.

2.2.6 In situ hybridization (ISH)

Prior to staining, dechorionated embryos were fixed at the desired developmental stage in 4% paraformaldehyde in PBS overnight at 4°C. The next day, embryos were dehydrated in methanol and kept at -20°C for at least 30 mins. For ISH, embryos were re-hydrated in PBS, refixed in 4% paraformaldehyde in PBS, and then prepared for ISH (Jowett and Lettice, 1994). Fluorescein- and digoxygenin-labelled probes were stained in blue using 1mg/ml NBT/BCIP (Roche) in NTMT (pH 9.5), or stained in red using Fast Red Tablets (Roche) dissolved in 0.1M Tris-HCl (pH 8.2). Antisense RNA probes against *ntl*, *hgg*, *pcdh18a*, *gsc*, *fzd7*a, *wnt11*, *dkk*, *chordin*, and *e-cadherin* were used.

2.2.7 Preparation of the genomic DNA and PAGE analysis

After microinjection, individual embryos (uninjected control embryos and CRISPR transient mutants) were processed for genomic DNA extraction. The standard PCR conditions were: 94°C for 5 min; 94°C for 30 s, 52°C for 25 s, 72°C 30 s for 35 cycles; and 72°C for 5 min, followed by denaturation for 3 min at 95°C. The PCR products were resolved by electrophoresis on non-denaturing polyacrylamide gels containing 15% acrylamide, 1X Tris-EDTA (TAE), 10% ammonium persulfate, and TEMED. After 2 h of electrophoresis at 120 V and 400 mA, the polyacrylamide gel was immersed in a 0.5% ethidium bromide solution for 10 min and then visualised.

2.2.8 Deep RNA sequencing and data analysis

Wild-type embryos were microinjected with 200 ng of Pcdh18a mRNA or 0.5 mM Pcdh18a MO. At 24 hpf, pools of 50 embryos from the wild-type and the injected clutches were collected. Total RNA extraction was performed with Trizol (Invitrogen) according to the manufacturer's protocol. The extracted total RNA samples were

tested on RNA nanochips (Bioanalyzer 2100, Agilent) for degradation. Sequencing libraries were generated with the TruSeq mRNA kit v.2 (Illumina). The size and concentration of the sequencing libraries were determined with DNA-chip (Bioanalyzer 2100, Agilent). Multiplexed samples were loaded on a total of six sequencing lanes. Paired end reads (2 × 50 nucleotides) were obtained on a Hiseq1000 using SBS v3 kits (Illumina). The sequencing resulted in 300 million pairs of 50-nucleotide-long reads. The reads were mapped against the zebrafish genome (Zv9) using TopHat version 1.4.1. Gene expression was determined with HTSeq version 0.5.3p3.

2.2.9 Cell culture methods

Cells were cultured in appropriate vessels (flask or culture dishes), under aseptic conditions and regularly subcultured when reaching 90% confluence. The cells were incubated and grown in sterile Cellstar cell culture dishes (Greiner Bio-One) of different sizes according to the experimental setup.

Maintenance of cells

Zebrafish Pac2 fibroblast cells were cultivated in Leibovitz's L-15 medium supplemented with 15% FBS, 1% Pen/Strep, 0.1% Gentamicin at 28 °C without additional CO_2 supply. To subculture cells, they were gently washed with PBS and detached with 0.25% trypsin-EDTA.

Human-derived cell lines (HeLa cells - Human ovarian cancer cell line and L-cells and L-cells stably transfected with E-cadherin-GFP) were cultivated in DMEM supplemented with 10% FBS and 1% Pen/Strep at 37 °C with 5% CO_2 supply. To subculture cells, they were gently washed with PBS and detached with 0.25% trypsin-EDTA.

Subculturing cells

To keep the cells at an optimum density, they were subcultured when reaching 90% confluence. The cell culture medium was removed by aspiration and the cells were

gently washed with PBS to remove traces of serum and salts. Afterwards, 0.25 % trypsin-EDTA solution was added and cells were incubated at RT. Detachment was monitored under the microscope and fresh growth medium was added to the vessel when 90% of the cells detached. Cells were collected in a conical tube and centrifuged at 500 x g for 2 mins. Cell pellet was resuspended in fresh growth medium and cells were seeded into new culture vessels.

Seeding cells

To determine the total number of cells in 1 ml, cells were detached, centrifuged and resuspended in fresh culture medium. 10 ul of cells were transferred onto a Neubauer counting chamber and counted by using a bright field microscope. Cell suspension was diluted according to the seeding density of the cell line and cells were distributed in new culture vessels.

Cryopreservation of cells

Cells were gently detached following the procedure used during subculturing and cell number was determined. Approximately 10^6 cells were resuspended in freezing medium (10% DMSO in FBS) and cells were aliquoted into sterile cryostatic vials. Aliquots were slowly frozen in an isopropanol containing box at –80 °C overnight and then immersed in liquid nitrogen.

Thawing cells

Cryovials were removed from liquid nitrogen and immediately placed in a 37°C water bath for 2 mins. Thawed cells were mixed with preheated growth medium and centrifuged at 500 x g for 2 mins. Cell pellet was resuspended in fresh growth medium and cells were transferred into new culture vessels. Cell growth was carefully monitored and growth medium was replaced after 24 hours.

Transient transfection of cells

Transient transfection of cells was performed using FuGene HD Transfection Reagent. 24 hours prior transfection, 5x 10^5 cells were seeded into 30mm dishes and cultivated until reaching 80% confluency. For transfection, 100 µl PBS, 1 µg plasmid DNA and 4 µl FuGene HD reagent were combined, shortly vortexed and spun down. The mixture was incubated for 15 mins at RT. In parallel, cells were washed once with PBS and fresh growth medium was added to the cells. Transfection mixture was added drop-by-drop to the dish and the cells were further cultivated for at least 24 hours depending on the experimental set-up.

Chemical treatment of cells

For the chemical treatment, cells were washed with PBS and treated with 1µM Dyngo4a (Tocris) for 24 hours before analysis.

Wound healing assay

Wound healing assays were performed using cell culture inserts (IBIDI). Approximately 5 x 10^4 cells were cultured in each cell culture reservoir, which was separated by a 500 µm thick wall. After 6 hours of cultivation, the culture inserts were removed and cell migration was monitored for several hours using an Axiovert 800 M inverted microscope. The obtained time lapse images were analysed using ImageJ software (NIH).

Western blotting

For Western blots, whole-cell extracts were prepared and resolved by 2-10% gradient SDS–PAGE. The proteins were then transferred to a PVDF membrane. The membrane was incubated with anti-GFP (Sigma, 1:1,000) and anti-PCNA (Abcam, 1:5,000) primary antibodies for 4 hours at room temperature. The bound antibodies were visualized with fluorescent dye-conjugated secondary antibodies (IRDye, Li-cor Biosciences) using an Odyssey Infrared Imaging System (Li-cor Biosciences).

2.2.10 Cloning of DNA fragments

Primers were designed with the help of the *Primer3* program (Rozen et al.,2000).

PRIMER NAME	SEQUENCE
Pcdh18aΔECD –mCherry Sp F1	5’ ATGGAGACTAGCAAGGGTACAGTGCT 3’
Pcdh18aΔECD –mCherry Sp R1	5’ TGCAGCCGTGGTGTACCCTGCCAATG 3’
Pcdh18aΔECD –mCherry F1	5’ ATGATCATCATTATCTCCCTTGGGGC 3’
Pcdh18aΔECD -mCherry R1	5’ TTAGCTCTGGCGTACGTCCTGAAGCA 3’
Pcdh18aΔICD-mCherry F1	5’ ATGGAGACTAGCAAGGGTACAGTGCT 3’
Pcdh18aΔICD-mCherry R1	5’ TTAGGAGACATCTAGAGGGCCGTCTCCA 3’
Frizzled7a antisense probe F1	5’ AGACCCAACCAGCAATTCAC 3’
Frizzled7a antisense probe R1	5’ CAGGTCTTCTCCCACTGCTC 3’
Wnt11 antisense probe F1	5’ CACGTCACTGAGCGTCATTT 3’
Wnt11 antisense probe F1	5’ ATCAGCCCACAGCTCTCACT 3’

2.2.11 PCR fragment purification and ligation

PCR was performed using Pfu DNA polymerase and PCR reaction was assembled according to the manufacturer’s protocol. PCR products were analysed on 1% agarose gels and appropriate bands were isolated from the gels using sharp blades. PCR fragments were purified using PeqLab Gel extraction kit, according to the manufacturer’s protocol. The eluted product was digested by the appropriate enzymes for further ligation into Pcs2+ vector backbone. Ligation was performed using T4 DNA ligase according the manufacturer’s protocol. 1 µl of ligation reaction was used for transformation into competent bacterial cells.

2.2.12 Transformation and plasmid preparation

For transformation, chemically competent TOP10® bacterial cells were used from

Invitrogen. Transformation was performed according to the manufacturer's protocol. 50 µl of transformation was spread on LB agar plates containing 100 µg/mL ampicillin and plates were incubated at 37°C overnight. Colonies were picked the next day, transfected into 5 mL LB medium containing 100 µg/mL ampicillin and incubated overnight at 37°C. The next day, the bacteria culture was transferred into Eppendorf tubes and centrifuged at 14,000 rpm speed for 5 min. Plasmid isolation was done by using Qiagen Midiprep kit solution.

2.2.13 Image acquisition

After ISH, embryos were mounted in 70% glycerol in PBS on slides. Images were taken on Olympus SZX16 microscope equipped with a DP71 digital camera using the imaging software Cell-A.

For confocal analysis, embryos were embedded for live imaging in 0.7% low-melting point agarose (Sigma) dissolved in 1x Ringer's solution. Confocal image stacks were obtained using the Leica TCS SP5 confocal laser-scanning microscope. We collected a series of optical planes (z-stacks) to reconstruct the imaged area. The step size of the acquired z-stack was 1 µm and was chosen based on the optimal z-resolution of the 63× objective with a numerical aperture of 0.9. The images were further processed using Imaris software 7.5 (Bitplane AG). Cell shape was measured using ImageJ software (National Institutes of Health) and approximately 100 cells from each group were analysed.

3 Results

The fine-tuning and precise coordination of cell behavior during morphogenesis is pivotal to proper embryonic development. Previous studies showed that mouse Pcdh18 is present throughout the embryo, particularly in the ventricular zone of the brain, in the heart and in the kidney (Homayouni et al., 2001). Previous studies have suggested that Pcdh18a might play a role in the organization of gastrula-stage embryos and contribute to correct positioning of tissues during development (Aamar and Dawid, 2008). In my thesis, I aimed to further characterize Pcdh18a and find the molecular mechanism underlying its involvement in early zebrafish development.

3.1 Dynamics of Pcdh18a expression during gastrulation

Using in situ hybridization, I first examined the spatiotemporal expression of Pcdh18a at various stages of early development (Figure 7). The zebrafish midline is best characterized by the expression of *notail* (*ntl*) in the presumptive notochord (Schulte-Merker et al., 1994) and therefore I used *ntl* as a reference point and to visualize the embryonic midline. I found that at 60% epiboly the *pcdh18a* domain is localized in the zebrafish midline, anterior to the notochord progenitors (Figure 7 a, asterisk). As gastrulation progresses, *pcdh18a* expression becomes more defined in the anterior midline (Figure 7 a', asterisk). In the next set of experiments, I also studied the expression pattern of key components of the pathway relative to the midline as non-canonical Wnt/PCP signaling has an important role during gastrulation. The transmembrane receptor *fzd7a* showed similar expression pattern to that of *pcdh18a* at 60% epiboly in the midline (Figure 7 b), however at later time points its expression was also detected in the lateral domains of the embryo (Figure 7 b'). The expression of the Wnt ligant *wnt11* was restricted to the embryonic margin at 60% epiboly and also at later stages (Figure 7 c, c').

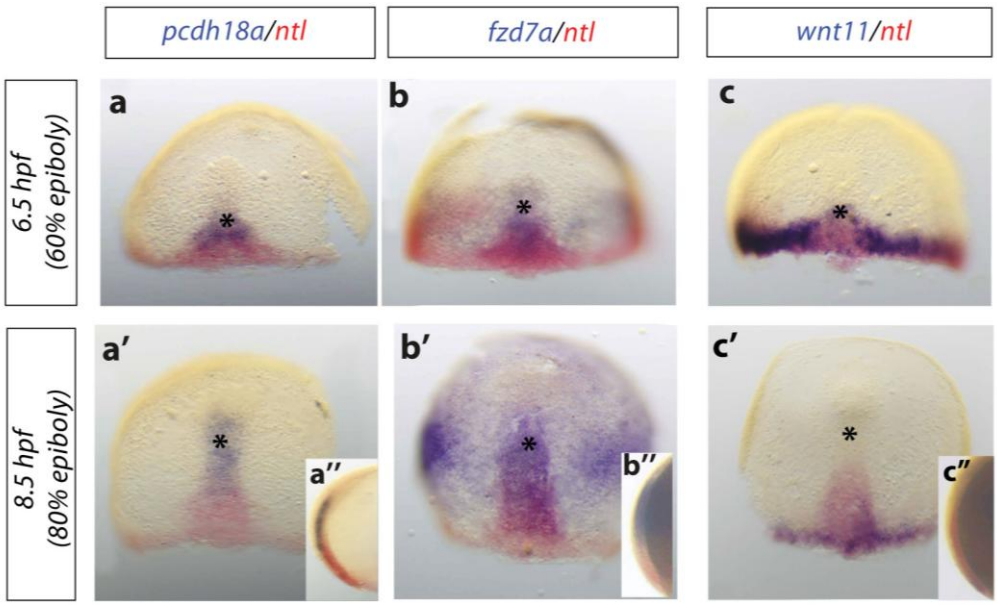

Figure 7 Pcdh18a labels the embryonic midline.

A whole mount double in situ hybridization approach, with pcdh18a (blue) and various markers (as indicated) (a-c'). Wild-type embryos were mounted with their prospective dorsal side upwards at two different stages (60% and 80% epiboly, 6.5 hpf and 8.5 hpf, respectively). Asterisk generally refers to the anterior midline.

pcdh18 is first detected at the beginning of gastrulation, at 60% epiboly (a, asterisk). Its localization is anterior to the forming notochord (marked by ntl), which becomes more distinctive as gastrulation progresses (a-a', asterisk). At 60% epiboly, two key components of the non-canonical Wnt/PCP pathway are expressed. fzd7a shows a similar expression pattern in the midline to pcdh18a (b). However, at 80% epiboly, its expression broadens to the lateral wings (b', asterisk). The key ligand of the PCP pathway, wnt11 is localized to the marginal zone of the embryo at 60% epiboly (c), and at a later time point with no expression in the anterior midline (c', asterisk).

To describe the expression of pcdh18a in the anterior midline in a more precise way, I used known markers of the prechordal plate (*goosecoid* (*gsc*) and *e-cadherin* (*e-cad*)), the anteriormost cell population in the zebrafish midline. I found that the pcdh18a positive cell cluster overlaps with the expression of *gsc* in the posterior prechordal plate (Figure 8 b). I further used the key cell-cell adhesion molecule *e-cad* as a precise marker for prechordal plate cells and found that Pch18a expression overlaps with *e-cad* domain (Figure 8 a).

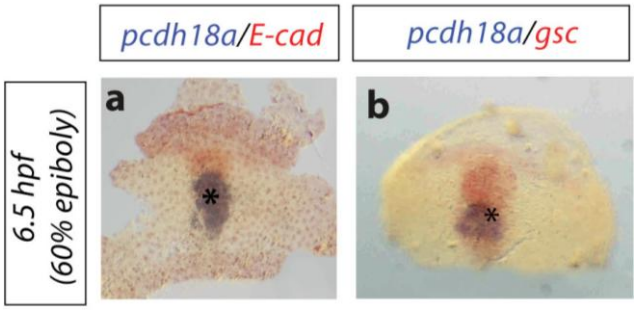

Figure 8 Pcdh18a expression overlaps with marker of the prechordal plate.

A whole mount double *in situ* hybridization approach, with *pcdh18a* (blue) and markers of the prechordal plate (as indicated). Wild-type embryos were mounted with their prospective dorsal side upwards at 60% epiboly, 6.5 hpf. Asterisk refers to the *pcdh18a* domain.
At 60% epiboly, *pcdh18* expression is detected in the midline and it partially overlaps with *e-cad* (a) and *gsc* (b), both markers of the prechordal plate.

Although *pcdh18a* previously showed a strong expression in the epiblast of gastrula stage zebrafish embryos (Aamar and Dawid, 2008), I observed the dominant expression of *pcdh18a* in the anterior midline, overlapping with markers of the prechordal plate progenitors. Therefore, I sought to find out whether *pcdh18a* is indeed localized to the epiblast, or rather labels cells of the hypoblast. To this end, I chemically blocked mesoderm formation in wild-type embryos from the sphere stage onwards, with a Nodal inhibitor (SB-505124) (Shen, 2007) and subjected them to *in situ* hybridization against *ntl* and *pcdh18a*. Embryos incubated with DMSO as a control developed properly, showing *ntl* and *pcdh18a* expression in the midline (Figure 9 a). Embryos in which mesoderm formation was blocked, exhibited complete loss of expression of *ntl* and I also observed the absence of Pcdh18a in the midline (Figure 9 b).

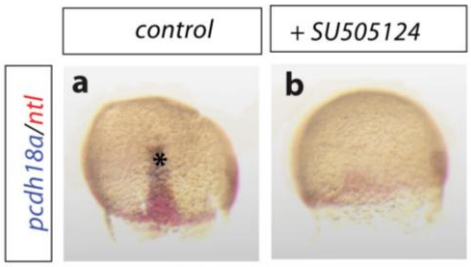

Figure 9 Nodal inhibitor treatment affects pcdh18a expression

Whole mount double *in situ* hybridization of wild type zebrafish embryos at 80% epiboly (8.5 hpf), stained for *pcdh18a* (blue) and *ntl* (red). Embryos were mounted with their prospective dorsal side upwards. Asterisk refers to the *pcdh18a* domain.
Zebrafish embryos were treated with 1% DMSO as a control (a,) and developed normally. Embryos treated with 30 μM of SU505124 (b) did not develop mesodermal structures as indicated by the absence of *ntl* in the midline. These embryos also lack the pcdh18a domain.

In conclusion, I identified *pcdh18a* as a marker of the posterior prechordal plate, overlapping with the expression domains of *e-cad*, *fzd7a* and *gsc*. I refer to this cell population as the notochord tip cells (NTCs). Further analysis revealed that *pcdh18a* expression is dependent on Nodal signaling and it rather labels hypoblast cells in the embryo. This observation was also supported by lateral sections of the embryo showing *pcdh18a* in deeper cell layers (Figure 7 insets).

3.2 Alterations in *pcdh18a* expression levels result in morphological abnormalities

To investigate the functional implications of pcdh18a expression in early stages, in the first instance, I suppressed Pcdh18a translation by using Morpholino oligonucleotides (Nasevicius and Ekker, 2000) and (Aamar and Dawid, 2008). Two different MOs were used: pcdh18a-UTRMO is complementary to the 5' UTR of the *pcdh18a* mRNA, while the sequence of the *pcdh18a* ATGMO blocked the translation initiation site.
In control experiments, no differences in development were detected (Figure 11). At 24 hpf, the two independent MOs produced the same phenotype; the embryos displayed developmental abnormalities, shorter body axis and bent tail (Figure 11). As both of the MOs induced the same phenotype, it is highly possible that their effect is specific and they target the same mRNA. Nevertheless, as a standard proof of MO

specificity, MOs are delivered in the one cell stage along with exogenous mRNA coding for the same gene however not containing a binding sequence for the MO. Thereby, exogenous mRNA could complement the effects of the MO injection and restore the wild type phenotype. *pcdh18a* mRNA contained a *pcdh18a* ATG MO binding site and therefore upon its delivery into the embryos, the co-injected MO would target and interact with the exogenous mRNA. This was evidence by an experiment where pcdh18a-GFP mRNA was injected along with pcdh18a ATG MO and those embryos showed no GFP signal (Figure 10).

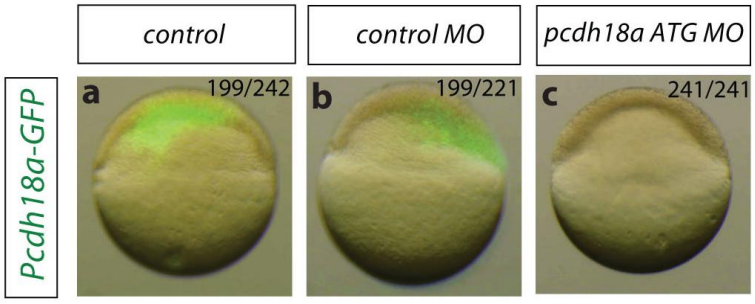

Figure 10 Pcdh18a ATG MO binds to pcdh18a-GFP in zebrafish embryos.

Embryos were microinjected in the one-cell stage with indicated constructs. Fluorescent images were taken at 5 hpf, Numbers at the upper right corner show affected/total number of embryos. Independence and p value were calculated by chi-square test. $p<0.0001$

Therefore to address the specificity of the MOs, I relied on *pcdh18a* UTR MO that did not carry a binding site for the synthetic *pcdh18a* mRNA. Interestingly, phenotypic changes induced by *pcdh18a* UTR MO injection could not be rescued by co-injection of *pcdh18a* mRNA (Figure 11, 20/35 - affected/total number of embryos).

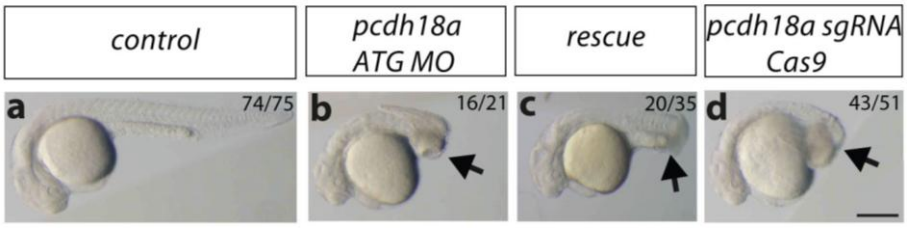

Figure 11 Pcdh18a is required for normal development of zebrafish embryos

Embryos were positioned laterally. Embryos were injected with indicated constructs in the one cell stage and were allowed to develop until 24 hpf and embryos were divided into two group: affected and non-affected embryos. Numbers in the upper right corner represent affected/ total number of embryos. In control: wild type phenotype / total number.

Pcdh18a morphants and CRISP-ants display severe malformations in the trunk and tail area at 24 hpf (arrows) as well as embryos injected with Pcdh18a MO and Pcdh18a mRNA, whereas the head seems unaltered. Independence and p value were calculated by chi-square test. $p<0.0001$
Scale bar=250 µm

As the specificity of the MO could not be entirely proven, I decided to employ a second approach in order to knock down pcdh18a function. In the light of new technologies, I used the CRISPR/Cas9 genome editing system that became increasingly popular to generate mutations in zebrafish (Hwang et al., 2013). As introduced in the Methods, I designed single-guide RNAs against the *pcdh18a* locus which were used in combination with Cas9 protein.

In the first instance, the specificity of the sgRNA was addressed in vitro. To do so, DNA templates of the *pcdh18a* coding sequence and a control sequence (GFP) was tested. Linearized DNA was incubated with *pcdh18a* sgRNA and Cas9 protein; and upon specific binding of the sgRNA to the target sequence; the DNA template was digested (Figure 12 a). To show that pcdh18a sgRNA could generate mutations in vivo, embryos were microinjected in the one cell stage with pcdh18a sgRNA and Cas9 protein and after 24 hours, the embryos were collected and as a fast readout, their genomic DNA was analysed by PAGE-based genotyping (Figure 12 b). Pcdh18a locus was amplified by PCR reactions and the migration of the PCR fragments was studied on a non-denaturing gel. Fragments that contain mismatches due the mutations melt at a different temperature and therefore migrate differently on the gel (Zhu et al., 2014). I detected such mismatches in the form of heteroduplexes suggesting that the *pcdh18a* sgRNA successfully targeted the *pcdh18a* locus. Injected embryos at 24 hpf also showed a similar phenotype to the MO-injected embryos, while the control injections resulted in no detectable malformations (Figure 11 d).

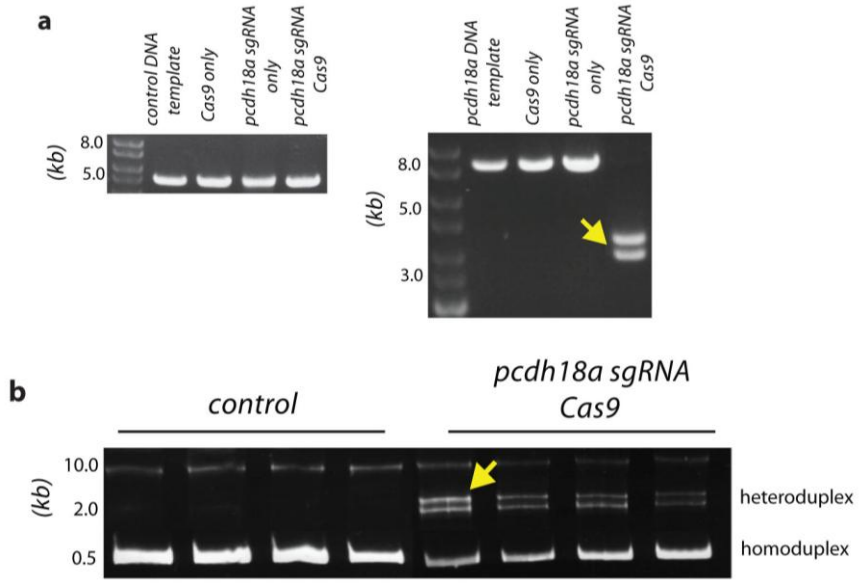

Figure 12 in vitro and in vivo analysis of pcdh18a sgRNA specificity

Plasmid containing the coding sequence for Pcdh18a or for GFP as control was used as a templates (a). pcdh18a sgRNA combined with Cas9 protein digested the pcdh18a containing template.
PAGE-analysis provided evidence that the specific gRNA generates mutations in the endogenous *pcdh18a* locus in zebrafish embryos (b). Homoduplexes and heteroduplexes (as a consequence of mismatching) of PCR products isolated from single control embryos and CRISPR/Cas9 injected embryos analysed on non-denaturing acrylamide-gels. Yellow arrow marks the heteroduplexes.

As both the MO injections and the CRISPR system resulted in similar phenotypes, I used these two approaches to address the functional role of Pcdh18a in early zebrafish development. The strong deformation in the trunk and tail regions suggested a compromised axial scaffold and such phenotypes have been shown to be a result of defective development during gastrulation (Hammerschmidt et al., 1996). I previously showed that *pcdh18a* is expressed in the posterior prechordal plate during gastrulation. For that reason, I investigated whether loss of *pcdh18a* affects the normal development of gastrula-stage embryos.

Possible impairment of the embryos was addressed by in situ hybridization of *ntl* at 9 hpf. The shape of the axial mesoderm labelled by *ntl* was altered; pcdh18a MO and CRISPR injected embryos displayed a wider body axis (Figure 13). The average width of the *ntl* domain in control embryos was 30 µm, while axis width in *pcdh18a* UTR MO and ATG MO injected embryos was increased to 51 µm and 46 µm, respectively. On average, transient CRISP-ants showed similar increase in the width of the ntl domain (45 µm). Similar phenotypes have been shown in embryos injected with

mRNA coding either for *e-cad* or *p120* catenin, a binding partner of e-cad (Babbs et al, 2004). These examples were used as a positive control in my set-up (Figure 13).

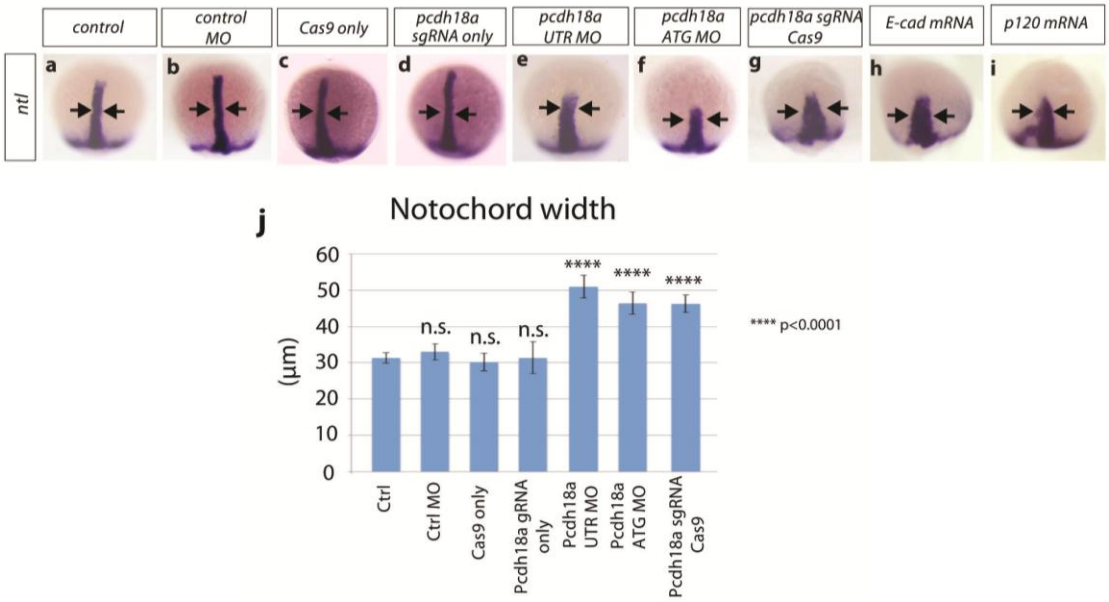

Figure 13 Early effects of the knockdown of Pcdh18a

in situ hybridization of zebrafish embryos injected with indicated constructs (a-i). Embryos were fixed at desired stage and stained against *ntl*. Embryos are mounted dorsally.

Loss of pcdh18a led to wider notochord indicated by a more dispersed *ntl* domain (e-g, black arrows) compared to the embryos injected with control constructs (a-d). E-cad and p120-ctn injected embryos showed similar phenotypes to the *pcdh18a* injected siblings (h-i).

Quantifications of the notochord width and length at 9hpf (j): Pcdh18a morphant and Pcdh18a CRISPant embryos developed a significantly wider notochord compared to the control embryos (Ctrl: 30 µm, UTR MO: 51 µm, ATG: 46 µm, CRISPR: 45 µm).

Student t-test *-p< 0.05, **** p<0.0001. The error bars represent the SEM.

The broader axial mesoderm at 9 hpf and the shorter axis at 24 hpf suggest impaired convergence and extension during gastrulation. To further confirm this hypothesis, I analysed the morphology of injected embryos after completion of gastrulation, at 11 hpf (Figure 14). In control embryos, the length of embryonic axis labelled by *ntl was* 200 µm, while pcdh18a ATG MO and CRISPR injected embryos developed a shorter axis (156 µm and 177 µm, respectively).

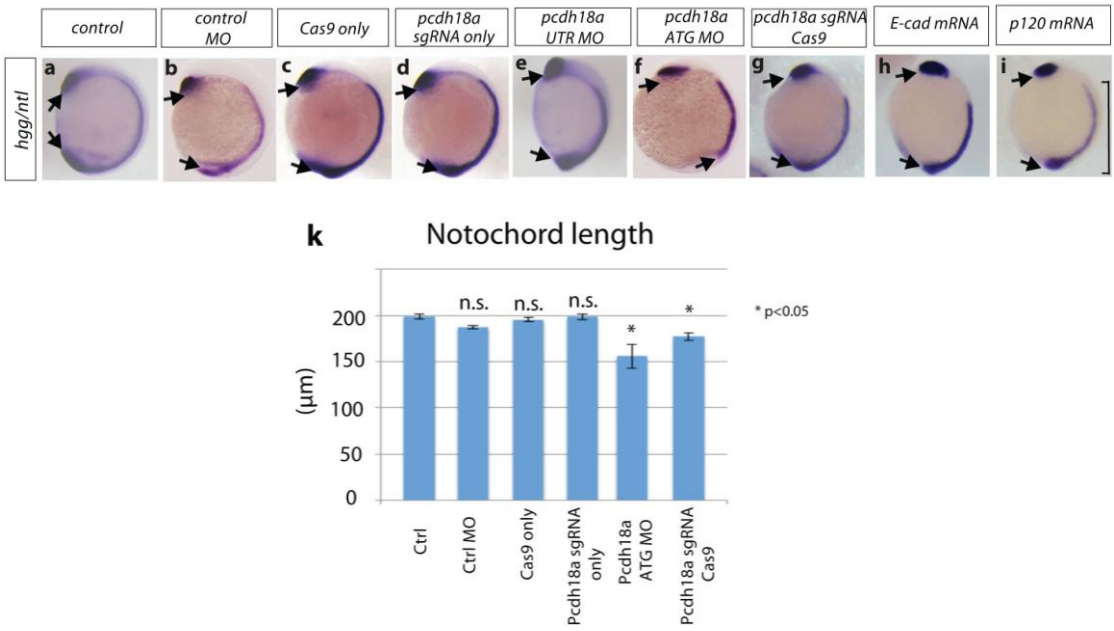

Figure 14 Effects of the absence of Pcdh18a on axis elongation

in situ hybridization of zebrafish embryos injected with indicated constructs (a-i). Embryos were fixed at desired stage and stained against *ntl/hgg*. *hgg* marks the anterior prechordal plate. Embryos are mounted laterally.

Loss of pcdh18a led to a shorter *ntl* domain wider notochord compared to the embryos injected with control constructs (a-e, black arrows). E-cad and p120-ctn injected embryos showed similar phenotypes to the *pcdh18a* injected siblings (h-i).

The embryo length was quantified (k) by measuring the length of the ntl domain from a dorsal view (scale set in i). Pcdh18a morphant and Pcdh18a CRISPant embryos developed a significantly shorter notochord compared to the control situations (Ctrl: 200 µm, UTR MO: 156 µm, CRISPR: 177 µm) respectively.

Student t-test *- 0.05, ****- 0.0001. The error bars represent the SEM.

Short and broad axial mesoderm are the characteristics of impaired cell movements during gastrulation (Solnica-Krezel and Cooper, 2002), and my observations suggest a similar effect in the loss of Pcdh18. As impaired movements are coupled with changes in cell behaviour such as cell shape, I sought to find out if loss of pcdh18a can affect the shape of notochord progenitor cells. I used gsc:GFP transgenic zebrafish in which not only the prechordal plate was marked by GFP expression but also the entire axial mesoderm (Dumortier et al, 2012). In these embryos, upon knockdown of Pcdh18a, the notochord progenitors showed a less compact organization in a medio-lateral

cross-section (Figure 15 b, c) and these cells were less elongated and displayed a more circular form in embryos with reduced Pcdh18a levels (Figure 15 e, f).

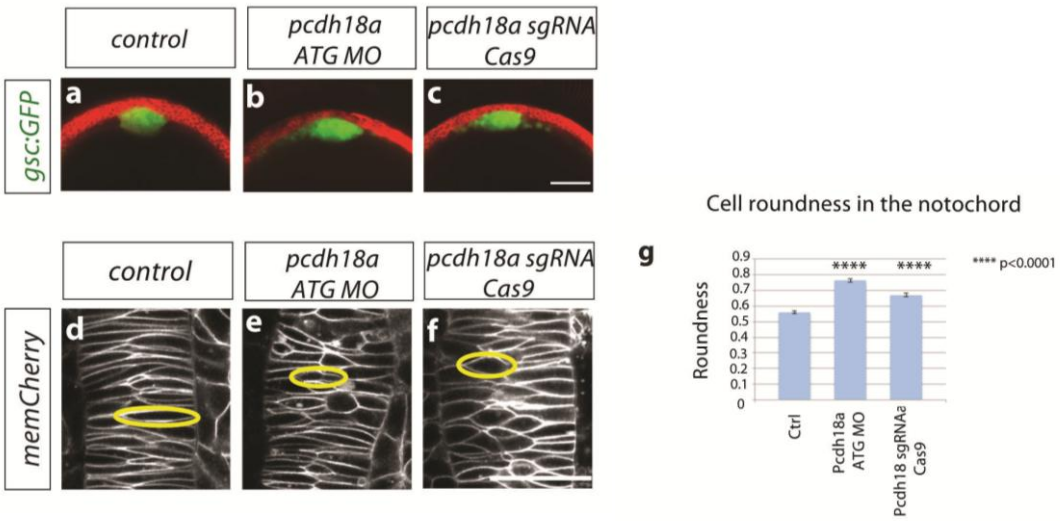

Figure 15 Pcdh18a affects notochord compaction

Analysis of the shape of the notochord in a cross-section of *gsc:GFP* transgenic embryos that were injected with the indicated constructs at 10 hpf (a-c). Scale bar, 100 µm.

Confocal microscopy-based analysis of cell shapes in the notochord of embryos at 12 hpf that were microinjected with the indicated constructs (cells with exemplary morphology were surrounded with a yellow circle) (d-f).

Quantification of cell roundness (g). Circularity (roundness) was measured using ImageJ software, in total of 100 cells in 10 different embryos of each tested construct. Circularity ranges from 0 (infinitely elongated polygon) to 1 (perfect circle). The ratio of cell extension medio-laterally and ap axis was quantified with student t-test. Student t-test ****- <p 0.0001. The error bars represent the SEM.

Scale bar, 100 µm.

In conclusion, I showed that Pcdh18a affects the behaviour of notochord progenitor cells and thereby influences the proper formation of the axial mesoderm. Nevertheless, it has been an intriguing observation as Pcdh18a showed no expression in the notochord progenitors. In the next step, I sought to investigate the influence of the loss of Pcdh18a positive cells on the organization of the trailing notochord progenitors. To do so, I designed an experiment independent of Pcdh18a knockdown in the embryo. By using a two-photon microscope, I ablated cell rows between the notochord progenitors and the Pcdh18a positive NTCs, thereby ablating connections between the two cell populations. After ablation, embryos were allowed to develop until the end of gastrulation and were then subjected to *in situ* hybridization against *ntl* (Figure 16 a', b').

In this set-up, gsc:GFP transgenic embryos were microinjected with a red tracer (nucleus marker) and cell rows were ablated at 7 hpf between the prechordal plate mesoderm and the NTCs as a control (Figure 16 a) or between the NTCs and the notochord progenitors (Figure 16 b). Ablation of the cells anterior to the NTCs did not lead to an obvious alteration in the morphology of the axial mesoderm (11/11 embryos). However, ablation of cells posterior to the NTCs led to the formation of a gap between the NTCs and the forming notochord (Figure 16, b, white arrow). These embryos displayed a shorter and broader axis, as shown by the expanded *ntl* domain (6/11). These observations suggest that the Pcdh18a-positive NTCs constitute a border cell cluster and provide an essential connection to the trailing notochord progenitors.

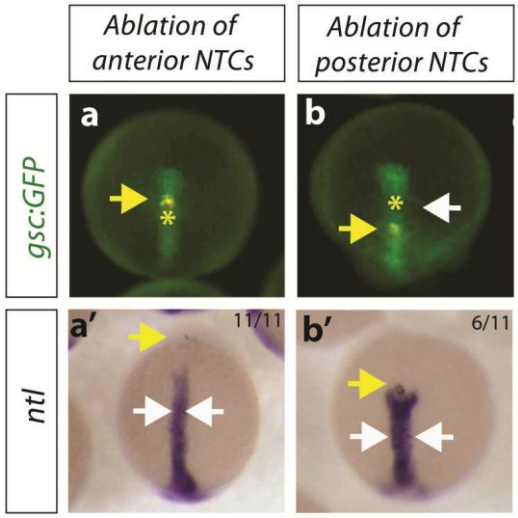

Figure 16 Physical connection of NTCs to the notochord progenitors is essential for proper notochord formation

Ablation of cell rows anterior (5th GFP positive cell row, a) or posterior (15th GFP positive cell row, b) to the NTCs in the *gsc:GFP* transgenic zebrafish embroys. Embryos were injected with a nuclear marker (Histone 2B-mCherry) and cell rows were ablated at 7 hpf using ultrashort laser pulses of a two-photon microscope. Yellow arrows mark the ablated cell rows. Asterisks mark the location of *pcdh18a*-positive NTCs.

Embryos were raised to 10 hpf, fixed, and subjected to ISH against *ntl*. Embryos develop an elongated notochord (11/11, a') when cells were ablated anterior to the NTCs, whereas the notochord progenitor cells move more slowly and a gap appears between the NTCs and the notochord progenitors upon ablation of a cell row in the posterior NTCs (b, white arrow). Consequently, the *ntl* expression domain remains shorter and broader (6/10, b').

3.3 Pcdh18a co-localizes with E-cad and affects its recycling

In order to characterize the mechanism by which Pcdh18a affects notochord progenitors, I first described the subcellular localization of Pcdh18a protein. In the absence of a zebrafish specific antibody for Pcdh18a, Pcdh18a-GFP construct was ectopically expressed in zebrafish embryos. Pcdh18a belongs to the cell-cell adhesion family of cadherins and as a transmembrane protein; its subcellular localization was detected in the cell membrane in a punctate manner and also in vesicles at 50% epiboly (Figure 17 arrows).

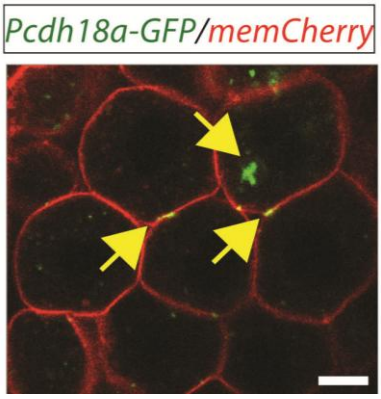

Figure 17 Subcellular localization of Pcdh18a-eGFP fusion protein at 50% epiboly in zebrafish embryos.

Confocal image of live zebrafish embryo injected with the membrane marker mCherry and Pcdh18a-GFP. Pcdh18a-GFP is localized in the membrane in a punctate manner and also observed in vesicles (yellow arrows)

Scale bar = 10 µm

As seen before, *pcdh18a* expression overlapped with the expression of *e-cad* and *fzd7a* in the prechordal plate and these proteins have been implicated in affecting gastrulation movements (Ulrich and Heisenberg, 2008). Therefore their co-expression with *pcdh18a* in the same cell population raised the question whether Pcdh18a interacts with these transmembrane proteins and whether this could serve as a possible mechanism of action of Pcdh18.

To investigate a possible interaction between these proteins in an *in vivo* environment, zebrafish embryos were microinjected with fluorescently tagged versions of these proteins and their subcellular distribution was analysed at sphere stage by confocal microscopy (Figure 18). I found that E-cad-GFP and Pcdh18a-mCherry co-localized

in cytoplasmic dots, and similar observations were obtained when Pcdh18a-mCherry was co-injected with Fzd7a-CFP. Interestingly, all three proteins co-localized in cytoplasmic vesicles. These experiments indicate that Pcdh18a might interact with E-cad and Fzd7a on a subcellular level. This raises the question whether their co-localization is specific to endocytic vesicles. In the first instance, I primarily focused on a possible interaction between Pcdh18a and E-cad.

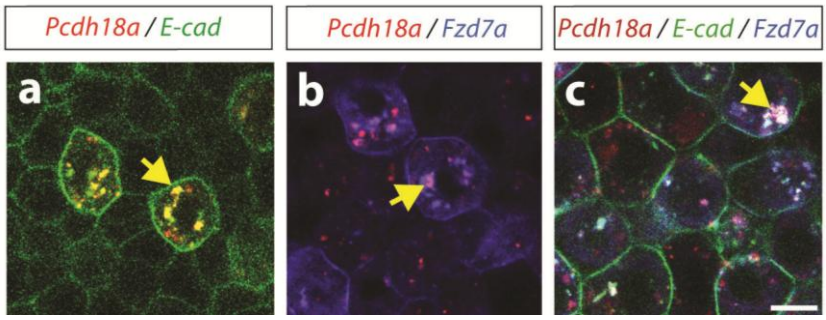

Figure 18 Pcdh18a co-localizes with E-cad and Fz7a.

Confocal images of zebrafish embryos at 5 hpf. Embryos were microinjected with mRNAs for the indicated constructs and were imaged *in vivo*. Pcdh18a is localized in the cell membrane and in endocytic vesicles, together with E-cad (a) and Fzd7a (b) or both (c). Yellow arrows indicate co-localization of the proteins.
Scale bar = 10µm

My previous observations led me to hypothesize that Pcdh18a might influence E-cad localization within cells. To test this theory, I first analysed whether E-cad containing vesicles are specific to compartments of the endocytic pathway. To do so, I performed fluorescent co-localization analysis of E-cad-mCherry in different Rab transgenic zebrafish lines. Rab GTPases regulate vesicular transport in endocytosis (Somsel Rodman and Wandinger-Ness, 2000) and such transgenic lines allow investigating E-cad distribution to endocytic vesicles in the absence and in the presence of Pcdh18a.
I injected E-cad-mCherry and Pcdh18a mRNAs into different Rab transgenic lines. At sphere stage, I monitored the subcellular distribution of E-cad-mCherry to the cell membrane and to Rab-labelled vesicles by confocal microscopy (Figure 19). To quantify whether E-cad associates with endosomes, the distribution of the fluorescently labelled proteins was statistically analysed by using Pearson's colocalizaion coefficient (PCC). Values near zero show no correlation between the

studied proteins while values near one would suggest high correction, with close to 100% co-localization.

I studied five different scenarios by using Rab5 and Rab11 to visualize the recycling endosomes, Rab 7 and Lamp1 to visualize the degradation pathway and a membrane marker to determine E-cad localization to the cell membrane (Figure 19). I found that E-cad distribution correlated with Rab5 and Rab11 positive endosomes in the presence of Pcdh18a, PCC=0.25 and 0.37, respectively. This difference appears to be significant compared to the distribution of E-cad in the absence of Pcdh18a (Rab 5 and Rab7 PCC= 0.16 and 0.24, respectively). Meanwhile, E-cad did not co-localize with Rab7 and Lamp1 in the absence of Pcdh18a, as evidenced by the low correlation coefficient values (PCC= 0.07 and 0.02, respectively). These co-localization values were not significantly altered upon Pcdh18a delivery to the embryo (PCC=0.09, 0.03, respectively). If Pcdh18a facilitates E-cad recycling, one would expect that its recycling to the plasma membrane would be similarly increased. I observed increased localization of E-cad in the cell membrane confirming my expectations (control and Pcdh18 presence, PCC= 0.2 and 0.32, respectively).

These observations suggest that Pcdh18a guides E-cad to the recycling pathway; hence influencing intracellular E-cad levels as well its presentation at the plasma membrane.

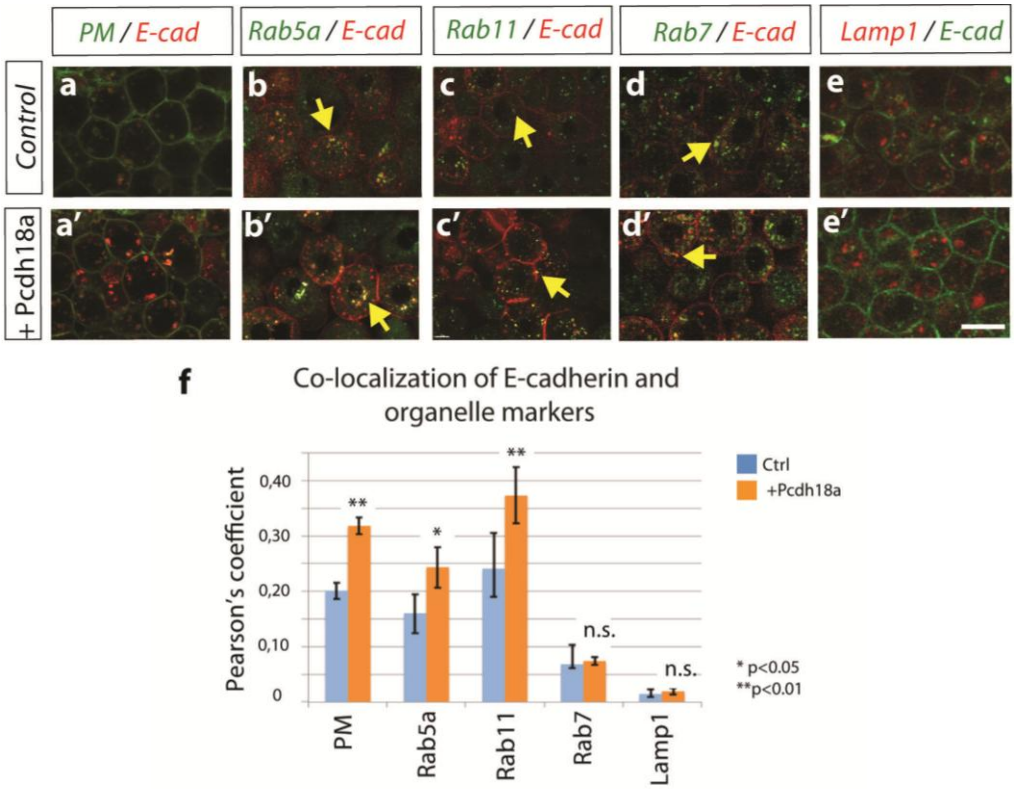

Figure 19 Endocytic routing of E-cadherin at 50% epiboly

Wild type embryos and Rab-transgenic embryos were microinjected with mRNAs for the indicated constructs (a-e') in the one-cell stage and embryos were imaged by confocal microscopy at sphere stage. Yellow arrows indicate E-cad localization with Rab proteins and Lamp1-positive vesicles. Pearson's co-localization coefficient was calculated from 70 µm thick confocal stacks of 5 different embryos of each scenario (f). Significance was calculated by Student's t-test. * p <0.05, ** p<0.01, n.s. –not significant. The error bars represent the SEM.

Cadherins can interact with each other by forming dimers at the surface of the same cell (lateral interaction) or at opposing cell surfaces (trans-interaction) thereby mediating the stability of cell-cell contacts (Perez and Nelson, 2004). My previous experiments were performed with the global overexpression of the fluorescently tagged constructs thus implicating a lateral interaction between E-cad and Pcdh18a. However, it is of interest to know whether Pcdh18a and E-cad are also in contact with each other on adjacent cell surfaces.

In the first instance, I examined whether Pcdh18a-Pcdh18a interactions occur on adjacent cell surfaces. Zebrafish embryos were microinjected at 8-cell stage with two differently labelled Pcdh18a mRNAs (GFP and mCherry) in two adjacent blastomeres (Figure 20 a). The embryos were imaged by confocal microscopy at sphere stage.

Pcdh18a-GFP and Pcdh18-mCherry show co-localization at the plasma membranes of the adjacent cells, which suggest that they are able to interact on neighbouring cell surfaces. This observation was further supported by the presence of Pcdh18a-GFP containing vesicles in the Pcdh18a-mCherry injected cells. This implicates that the interaction of the two proteins at the plasma membrane resulted in the endocytosis of the complex.

In a similar set-up I sought to find out whether Pcdh18a and E-cadherin also co-localize on adjacent surfaces. Although I did not see observe their association at the cell surface, cytoplasmic vesicle containing E-cad and Pcdh18a was detected in Pcdh18a injected cells. This indirectly suggests that the two proteins interacted at the cell surface, which resulted in the internalization of the complex (Figure 20).

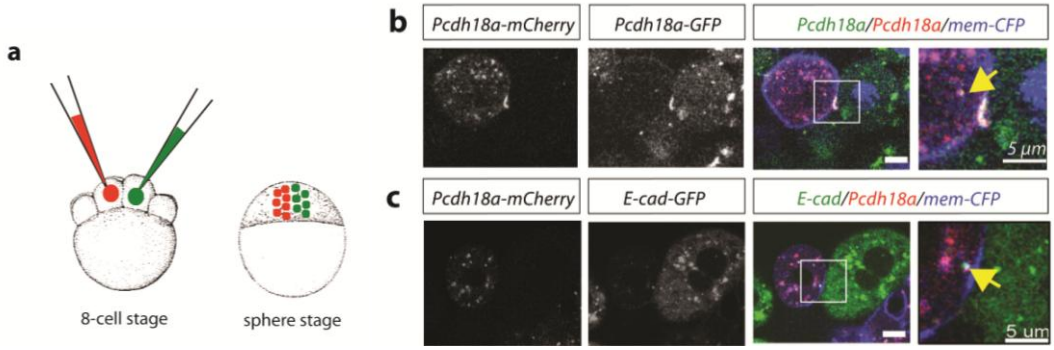

Figure 20 Pcdh18a and E-cad -interactions on adjacent blastomeres in zebrafish embryos

Experimental set up of the clonal injection (a).At the 8-cell stage, the embryos were injected *pcdh18a-mCherry* and *mem-CFP* mRNAs in one blastomere (red) and *pcdh18a-GFP or e-cad-GFP* mRNA (green) with a blue nucleus marker in an adjacent blastomere. At sphere stage, embryos were analysed by confocal microscopy.

Interaction of the Pcdh18a proteins on adjacent cell surfaces was detected, as well as the internalization of the complex (b). Inset shows co-localization at higher magnification, yellow arrow marks cytoplasmic vesicles.

Endocytosis of Pcdh18a/E-cad was observed in Pcdh18a containing cells (c). Inset shows co-localization at higher magnification, yellow arrow marks cytoplasmic vesicles.

(Scale bar = 10 µm, inset scale bar= 5 µm).

These observations confirm that Pcdh18a associates with E-cad and with Pcdh18a on adjacent cell surfaces. Moreover, this interaction can also lead to the simultaneous endocytosis of these proteins (Figure 20, insets). These experiments also imply that

the endocytosis of the Pcdh18a protein complex could be triggered by the interaction of their extracellular domain.

To study the contributions of the different domains of Pcdh18a to endocytic trafficking of E-cad *in vivo*, I used full length and deletion constructs of Pcdh18a in combination with fully functional E-cad (Figure 21).

I first validated the subcellular localization of the Pcdh18a deletion constructs. I first designed and constructed two different forms of Pcdh18a: Pcdh18aΔICD lacks the entire intracellular domain of Pcdh18a and the domain itself was replaced by an mCherry fluorescent tag. Pcdh18aΔECD lacks the entire extracellular domain except the signal peptide that directs the protein into the plasma membrane. The EC domain was replaced by an mCherry tag (Figure 21).

Zebrafish embryos were injected in the one-cell stage with different constructs of Pcdh18a, together with a membrane marker and embryos were imaged by confocal microscopy at sphere stage (Figure 21).

The fully functional Pcdh18a is localized to the plasma membrane in a punctate manner and present in endocytic vesicle (Figure 21). Pcdh18aΔECD showed similar distribution suggesting that the absence of the extracellular domain did not affect Pcdh18a localization. On the contrary, Pcdh18a-ΔICD mainly localized to the plasma membrane (Figure 21 b). My observations were confirmed by the analysis of their localiztaion along the plasma membrane, shown by intensity histograms. Full length Pcdh180 as well as Pcdh18aΔECD did not correlate with the membrane marker, whereas Pcdh18a-ΔICD did show association with the cell surface (Figure 21). This analysis suggests that it might be the intracellular domain of Pcdh18a, which is required for its proper localization.

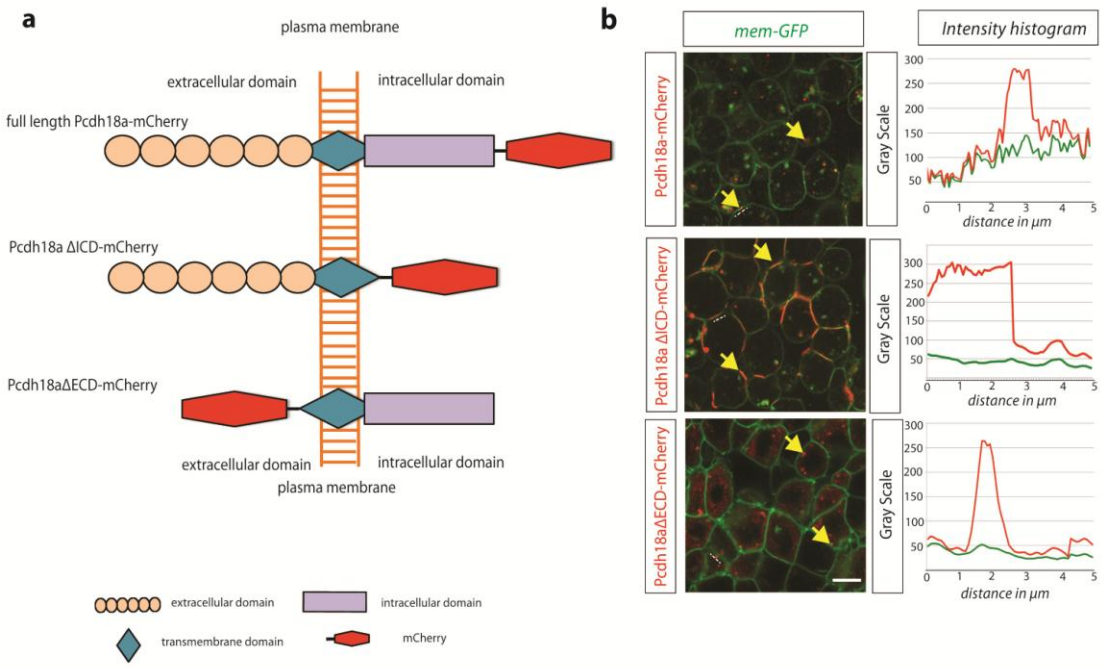

Figure 21 Subcellular localization of Pcdh18a deletion constructs

Design of the deletion constructs (a). In vivo test of the subcellular distribution of the deletion constructs. At the one-cell stage, the embryos were injected mRNA of indicated constructs together with a membrane marker and were imaged at sphere stage by confocal microscopy.
Their distribution in the membrane was further assessed by creating intensity histograms, showing that Pcdh18aΔICD is ubiquitously expressed in the cell membrane, with Pcdh18aΔECD and full-length proteins show similar distribution, association to the membrane and to cytoplasmic vesicles (yellow arrows). The histogram represents one segment of the membrane containing the injected constructs.
(Scale bar = 10 µm)

As Pcdh18aΔICD showed an unexpected distribution in the cell membrane, in the following I examined its effects on Pcdh18a and E-cad distribution. I injected zebrafish embryos with the combination of these proteins and imaged their distribution at sphere stage (Figure 22).
Co-expression of full length Pcdh18a and Pcdh18aΔICD in the same cells resulted in the endocytosis of Pcdh18a-ΔICD suggesting that the intact IC domain of the full length Pcdh18a was sufficient to induce internalization (Figure 22 a b). Interestingly, Pcdh18aΔICD was not able to lead to the endocytosis of E-cad, as shown by the lack of E-cad/Pcdh18a containing vesicles (Figure 22 c d).

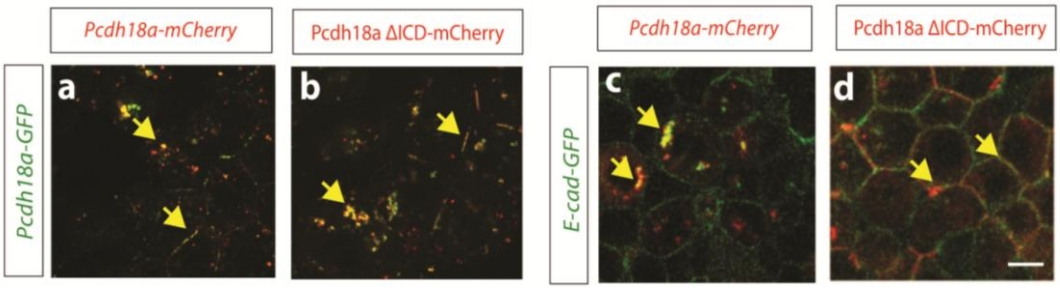

Figure 22 Pcdh18a cytoplasmic domain is necessary for endocytosis

Confocal images of zebrafish embryos at 50 % epiboly. Embryos were injected with indicated constructs at the one-cell stage.
Full-length Pcdh18a proteins co-localize in the cell membrane and in the cytoplasm (a). As previously seen, Pcdh18aΔICD was mainly located in the plasma membrane (Figure 23), however upon adding full length Pcdh18a (b), it was endocytosed.
Full length Pcdh18a co-localizes with E-cad in endocytic vesicles, however this was not observed in the co-expression of Pcdh18a-ΔICD and E-cad.
Scale bar =10 µm

This observation implies that the absence of the intracellular domain of Pcdh18a negatively affects E-cad endocytosis and recycling.
In summary, I conclude that Pcdh18a influences E-cad trafficking *in vivo*. My data suggest that E-cad levels rise in the membrane in the presence of a fully functional Pcdh18a protein and Pcdh18a also affects the endocytic routing of E-cad. Co-localization of these proteins was observed both at the same and opposing cell surfaces.

3.4 Remodelling of E-cad adhesion complexes determine cell migration

Based on my previous experiment, Pcdh18a seems to have a significant influence on E-cad distribution. This alone implies that Pcdh18a-directed rearrangement of E-cad within the cell would lead to changes in cell behaviour, particularly in migratory capacity. E-cad has been long recognised as a protein with fundamental impact on cell migration (Campbell and Casanova, 2015).
To address the question whether Pcdh18a alters migratory behaviour of cells, I performed a wound-healing assay. I used human cervical cancer cells (HeLa) as they

display low endogenous expression of E-cad (Hazan et al., 2004). Therefore, they are perfect models to simultaneously analyse the function of key players of zebrafish gastrulation *in vitro*.

To examine the migratory behaviour of HeLa cells in culture, cells were transfected with E-cad, Pcdh18a or the combination of these proteins (Figure 23). Pcdh18a alone did not affect migration speed compared to the control population (11 μm/hour migration speed average in both control and Pcdh18 transfected cells). As E-cad holds cells together, the motility of E-cad positive cells was significantly decreased (6 μm/hour). Notably, Pcdh18a sped up migration of E-cad positive cells to levels comparable to control cells (12 μm/hour).

It is known that PCP signalling positively affects migratory behaviour (Ulrich et al, 2005). To analyse the effects of PCP signalling on cell migration, cells were transfected in the same scenarios in combination with Fzd7a.

Fzd7a-positive HeLa cells and Pcdh18a/Fzd7a-positive HeLa cells moved into the cleft significantly faster than the control cells (21 μm/hour and 18 μm/hour, respectively, Figure 23). Surprisingly, Fzd7a and E-cad positive cells showed reduction in their migration (7 μm/hour) suggesting that Fzd7a alone could not rescue the E-cad slow migrating phenotype. On the other hand, transfection of Pcdh18a in combination with Fzd7a and E-cad resulted in the fast migration of the cell population, exceeding the speed of control cells (14 μm/hour).

I conclude that E-cad negatively, while Pcdh18a and Fzd7a positively affect migration speed into the wound. Furthermore, Pcdh18a but not Fzd7a could overcome the effect of E-cad.

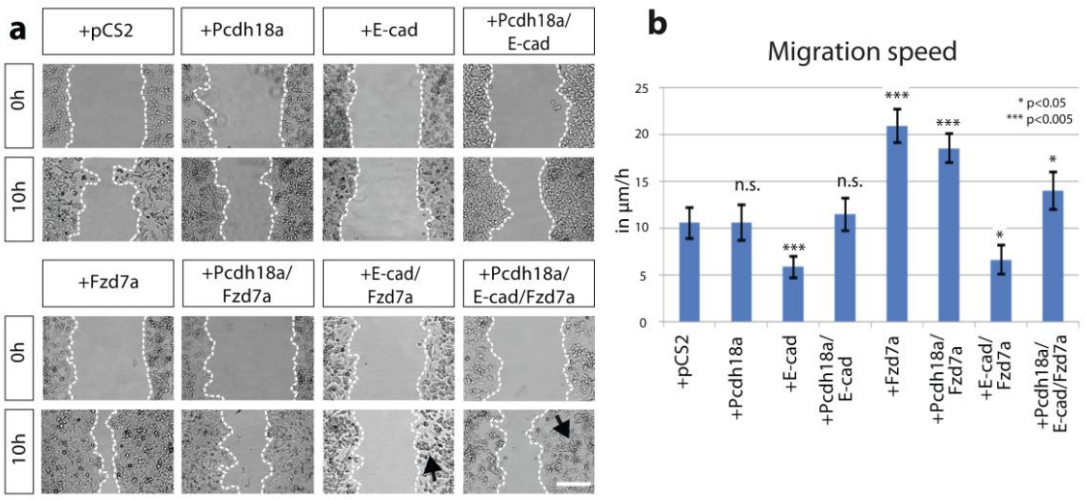

Figure 23 Pcdh18a affects cell migration in an E-cad-dependent manner

Wound-healing assay in HeLa cells (a). Cells were transfected with the indicated constructs, seeded into Ibidi culture inserts and allowed to adhere. Inserts were then removed, thus creating a gap between the cell populations. Similarly to scratch assays, the migratory behaviour of cells into the wound was monitored for 10 h. Arrows mark cell clusters, and the dotted line shows limits of the confluent cell layer. (Scale bar = 200µm)

Quantification of the migration speed of HeLa cells (b). The experiments were conducted in triplicates. Significance was calculated by using Students t-test. * <0.05; ***<0.005

To further test whether the observed changes in the migratory behaviour were caused by the endocytic routing of E-cad, I blocked endocytosis in mouse fibroblasts (L-cells), stably expressing E-cad-GFP using 1 µM Dyngo4a, an inhibitor of clathrin-mediated endocytosis. Similar to my previous experiments with HeLa cells, Pcdh18a expression increased cell migration in E-cad-GFP^{+} L-cells (8 µm/hour, Figure 24). However, reduced endocytosis led to decreased cell migration (3 µm/hour, Figure 24). This decrease was partially compensated by Pcdh18a expression; although did not reach migration speed comparable to untreated cells (Figure 24).

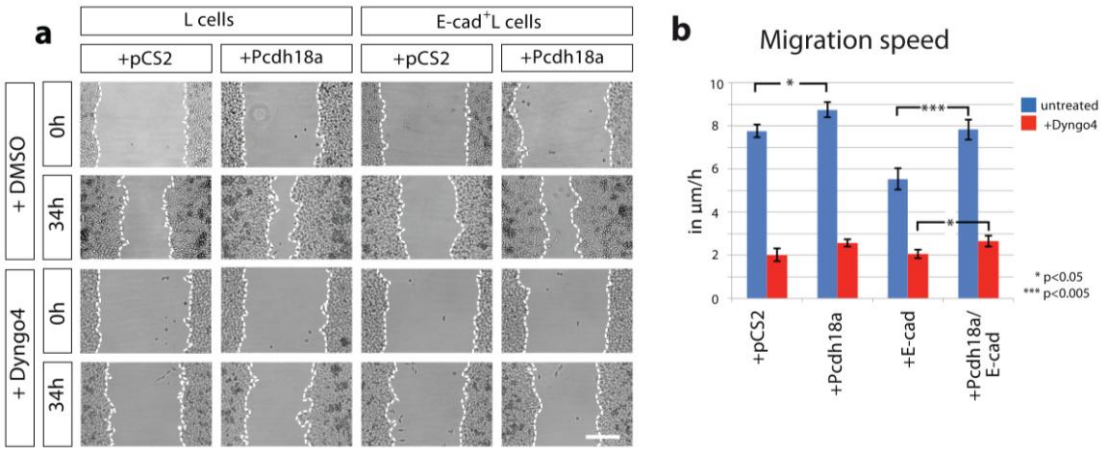

Figure 24 Blockade of endocytosis affects Pch18a dependent cell migration

Wound-healing assay in L-cells (a). The migratory behaviour of the cells was monitored for 34 h. Cells were transfected with indicated constructs and treated with 1%DMSO or 1 µM Dyngo4a, an inhibitor of endocytosis. (Scalebar = 200 µm)

Quantification of the migration speed of L-cells after blocking endocytosis (b). The experiments were conducted in triplicates. Significance was calculated by using Students t-test. * <0.05; ***<0.005

Remodelling of cell-cell adhesion is key to migrating cell populations and my analysis revealed that Pcdh18a can convert a slow migrating cell group into fast migrating one, by influencing E-cad recycling. As migration of cells is also controlled by the preferential localization of membrane proteins in the leading or trailing edge of cells, I sought to find out to which part of the cell membrane Pcdh18a preferentially localizes. I found that in zebrafish embryos, Pcdh18a was mainly localized to the posterior cell surfaces (67%) in the notochord tip cells (Figure 25). Interestingly, in individual zebrafish Pac2 fibroblasts, Pcdh18a was localized to protrusions (Figure 25). This suggests that Pcdh18a might also play a role in cell interactions by being localised to protrusions. However, detailed characterization of such protrusions will be necessary to draw further conclusions regarding the role of Pcdh18a in this context.

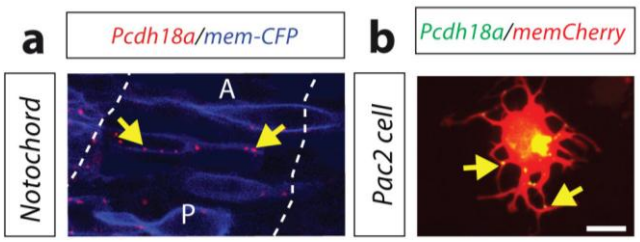

Figure 25 Pcdh18a is localized to protrusion and to the posterior cell surface

In Pac2 fibroblasts, Pcdh18a-GFP is localized in protrusions (a). The mosaic expression of Pcdh18a-mCherry in the NTCs shows that Pcdh18a is preferentially localized in the posterior region (c) (a=67%, p=24%, n=8 cells in 5 embryos) of the developing zebrafish embryo at 6 hpf.
Scale bar, 10 µm.

3.5 Pcdh18a positive tip cells shape the notochord

My previous results suggest that a cell population in the posterior prechordal plate– the notochord tip cells are required for the structural organization of notochord. This observation was further supported by the improper extension of the axial mesoderm when cell rows between the NTCS and the notochord progenitors were ablated (Figure 16). At a molecular level, Pcdh18a changes the migratory behaviour of these cells by affecting E-cad recycling (Figure 19, Figure 24). These altered adhesive properties result in the insufficient elongation and intercalation of the notochord progenitors. This implies that the anteriorly located NTCs might pull the notochord progenitors forward and thereby lead to the stacked alignment of cells that characterizes the axial mesoderm.

To experimentally address possible forces exerted by NTCs is extremely difficult and cell culture experiments on single cells would not necessarily reflect situations within the embryo. Therefore, we developed a simulation in collaboration with physicists in order to mimic the organization of the mesodermal tissue and to analyse it in a quantitative way (Figure 26)

We implemented a lattice-based mathematical model called Cellular Potts Model (CPM), which well represents the experimentally available cell properties (Graner and Glazier, 1992). Cells move and shape their change according to the predefined parameters (A complete list of equations and parameters is available in the Appendix, **Error! Reference source not found.**Figure 32) Based on the different characteristic of mesodermal cells within embryo relative to their position, we specified four

different cell populations: the leading prechordal plate cells (PPM), the notochord tip cells (NTC), the notochord progenitors, and the surrounding lateral plate mesoderm (LPM). The adhesive and migratory properties of NTCs were adjusted in three different set-ups (Figure 26).

In the first scenario, NTCs exhibit high migration speed without strong intercellular connections and such migration would result in an abnormally shaped notochord (Figure 26). The notochord progenitors did not converge properly to the midline and simultaneously failed to elongate along the defined anterior-posterior axis. The NTCs exhibited an oblong shape that was perpendicular to the AP axis.

In the second scenario, NTCs were highly connected by strong cell-cell adhesion. It also caused aberrant cellular architecture within the axial mesoderm (Figure 26). The shape of the prechordal plate was concave and did not resemble the in vivo situation. This observation indicates that strong adhesion within the NTCs not only inhibits the elongation of the notochord, but also influences the proper migration of the prechordal plate. This outcome was consistent with my previous experiments in which embryos had reduced levels of Pcdh18a and showed a short and broad notochord (Figure 13). In the third scenario, high cell-cell adhesiveness and cell motility were assigned to the NTCs. In this case, the prechordal plate acquires a convex outline, which resembles the shape of the PPM in the in vivo situation and the notochord progenitor properly aligned along the AP axis.

In summary, this simulation revealed that both the strong cell-cell adhesion and high migratory capacity of notochord tips cells are important features to the proper formation of the chordamesoderm (Figure 26).

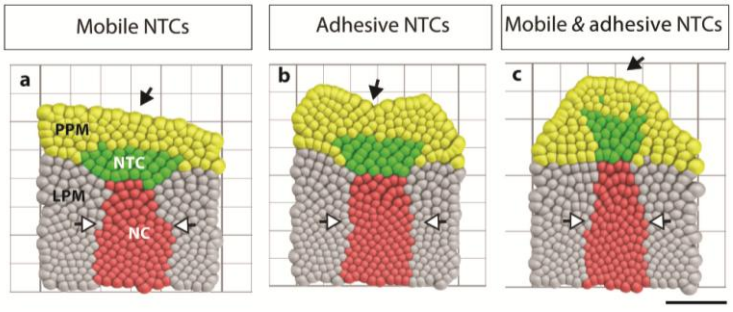

Figure 26 Simulation of cell movements during gastrulation

NTCs were given different properties: high motility (a), high adhesiveness (b) or high motility combined with strong adhesion (c) relative to the neighbouring tissues. White arrows marks the width of the axial mesoderm, while black arrows highlight the shape of the prechordal plate

PPM – prechordal plate mesoderm, LPM – lateral plate mesoderm, NC – notochord, NTC – notochord tip cells
Scale bar= 100μm

3.6 Pcdh18a affects cell migration in vivo

The results of the simulation and cell migration assays suggested that Pcdh18a affects the migration of cells in an adhesion-dependent manner. It further implies that a highly migratory and adhesive cell population positively influences the organization of the following cell population. To experimentally validate this theory, migration of small cell clones was monitored in the zebrafish embryo. I injected embryos at the one-cell stage with either Pcdh18a mRNA or E-cad mRNA and at shield stage; cells deriving from the lateral mesoderm were transplanted into the lateral mesoderm of a wild type host embryo. The migration and organization of such clones was then monitored until 80% epiboly (Figure 27).

In a control situation, the transplanted wild type cells dispersed over time and moved further away from the marginal zone of the embryo. However, they did not show an organized movement towards the animal pole (Figure 27a). Interestingly, Pcdh18a positive clones migrated in an organized fashion and the shape of this structure resembled a rod-shaped notochord (Figure 27b). Further sectioning of these embryos also revealed that this organised structure consists of a more compact cell population in comparison to the control situation (Figure 27).

As E-cad mediates strong cell-cell adhesion, E-cad positive cell clusters displayed round shape and migrated slowly towards the animal pole, which are consistent observations with the wound –healing assay (Figure 23). We sought to find out whether blockade of endocytosis *in vivo* would also lead to the reduced migration of cells as it did in the wound-healing assay. Pcdh18a expressing cell clones, in which endocytosis was blocked with a dominant negative form of Dynamin, did compact, however, the cluster did not migrate towards the animal pole.

E-cad shows a ubiquitous expression pattern throughout the zebrafish embryo; with stronger domains in the prechordal plate and notochord tip cells (Figure 8). Therefore, these observations on the compaction of the cells are consistent with the results of the migration assay where Pcdh18a sped up the migration of E-cad expressing cells (Figure 23).

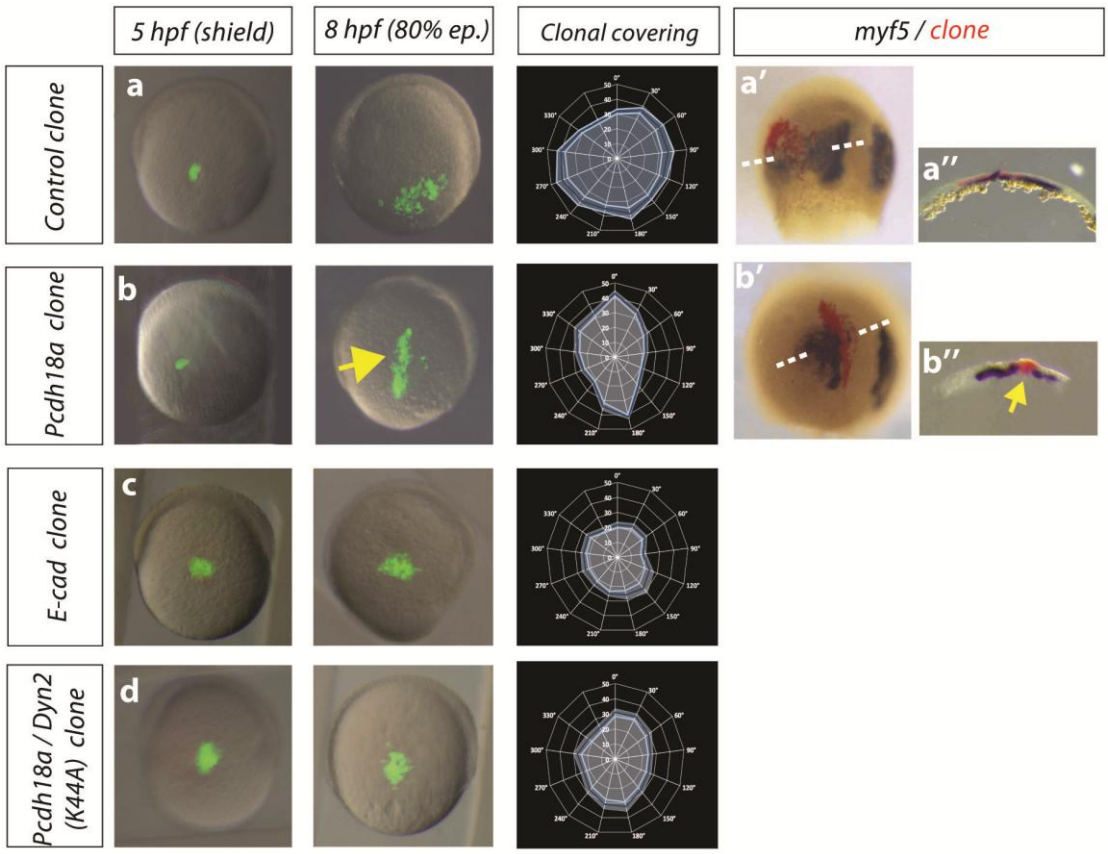

Figure 27 Pcdh18a positive clones move as an organized cohort towards the animal pole.

Embryos were microinjected with mRNAs for the indicated constructs. At 5 hpf, approximately 50 cells were grafted into the lateral embryonic margin of uninjected host embryos. The embryos were allowed to develop to 8 hpf when the migration and the directionality of the cell clusters were analysed and displayed in a wind rose plot. Animal pole was set to 0°, vegetal pole was set to 180°. Blue line indicates mean value of clonal coverage measured in ten different embryos per experiment and white lines indicates SEM. Yellow arrow marks the elongated (b) and compact clone (b'')
After microinjection and transplantation, the embryos were fixed and subjected to in situ hybridization for the LPM marker *myf5* (a', b'). Horizontal cross-sections (marked by the dashed line) revealed the formation of an ectopic rod-shaped structure of the Pcdh18a-positive clones in the LPM (a'', b'').

Based on these results, I conclude that Pcdh18a is required for the collective migration behaviour of cells in the NTCs and it also leads to the compaction of this cell population. As shown in the transplantation assay, Pcdh18a positive cells organized into a rod-shaped structure. However, this raised the question whether the ectopic expression of Pcdh18a in cell clones could also lead to the formation of a secondary axis.

To experimentally address this question, cell clones with different Pcdh18a or E-cad levels were transplanted at the onset of gastrulation into the zebrafish lateral plate

mesoderm (Figure 28) and the embryos were allowed to develop to the end of gastrulation, and fixed and stained against *ntl* to mark the notochord.

I found that Pcdh18a positive cell clones were not able to induce ectopic expression of the notochord marker *ntl* (Figure 28 b). In contrast, Chordin/Dkk1 positive clones, which are known to generate a secondary organizer, could induce a secondary notochord (Figure 28).

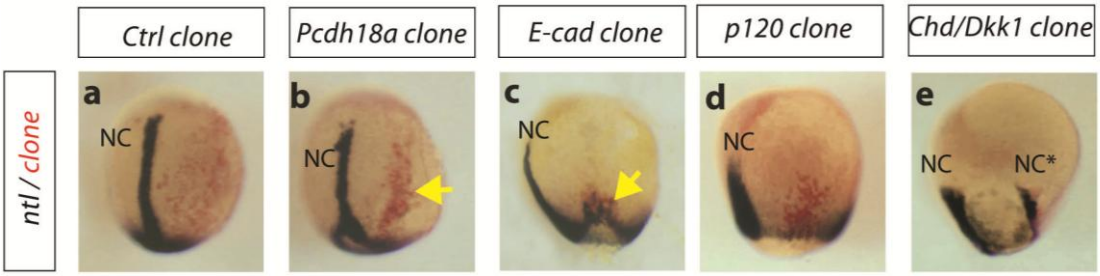

Figure 28 Pcdh18a is not able to induce a secondary axis

Transplantation analysis of zebrafish embryos at 5hpf. Donor embryos were injected in the one cell stage with indicated constructs and a lineage tracer (in red). Cells were transplanted into a host embryo in the lateral plate mesoderm. The embryos were allowed to develop to 90% epiboly, then fixed and subjected to in situ hybridization against *ntl*. Yellow arrows indicate the cell clones.

To further provide evidence that Pcdh18a alone could not induce the formation of a secondary axis, transcriptomics analysis of Pcdh18a-overexpressing embryos, Pcdh18a-morphant embryos and wild types was performed (Figure 29). In concordance with the previous results, no significant alteration in the expression of mesodermal genes such as *chordin, gsc*, *ntl, shh a*, and *shh b*, or in the expression of *e-cad* and *fzd7a* was seen (Figure 29) showing that although Pcdh18a organizes cell populations it does not affect gene expression. It rather influences cell behaviour via E-cad mediated endocytosis.

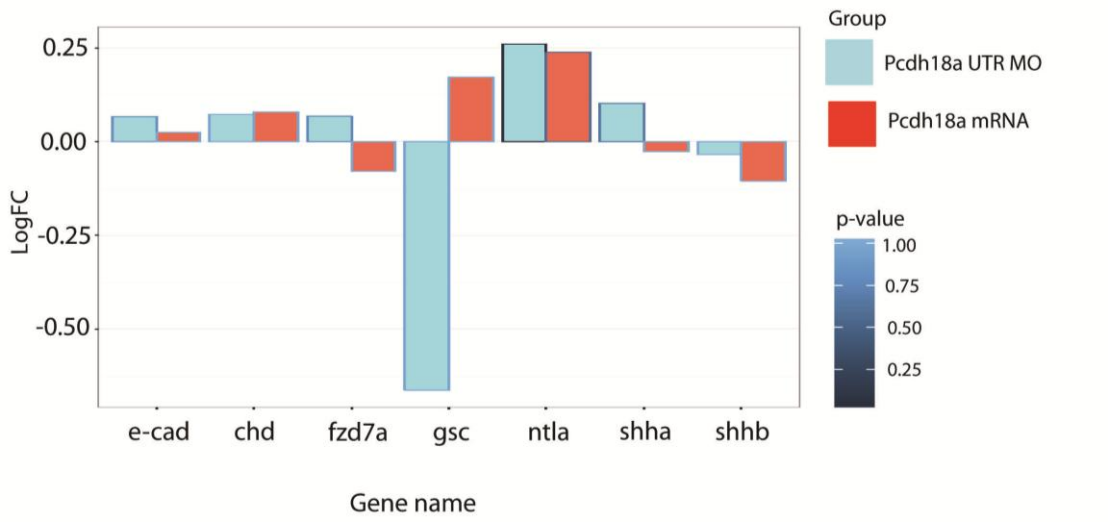

Figure 29 Pcdh18a does not affect gene expression

Transcriptional profiling of zebrafish embryos expressing Pcdh18a mRNA (red) or Pcdh18a UTR MO (blue) at 24hpf. Expression levels of genes influencing organizer formation or axis induction (i.e. *goosecoid*, *shh*. *chordin*), was not altered significantly. Similarly, *e-cad* or *fzd7a* expression showed no alterions. P-value is indicated in the column borders

In conclusion, this work has identified Protocadherin18a (Pcdh18a) as an essential player in the organization of the zebrafish axial mesoderm.

The gene has a distinct expression domain in the axial mesoderm and its misexpression leads to severe malformations in the trunk and tail of the developing embryo. This alone suggests a fundamental role for Pcdh18a in cellular rearrangements and essentially mesoderm organization during gastrulation.

In-depth analysis revealed that Pcdh18a interacts with E-cadherin, a classical cell-cell adhesion protein in the anterior axial mesoderm and leads to its endocytosis and subsequent recycling to the cell membrane. Through such mechanism, Pcdh18a can control E-cadherin levels in the cell membrane thereby affecting adhesive junctions and promoting cell migration.

Through a mathematical simulation we were able to model the migratory behaviour of cells within the mesodermal sheet of a gastrula embryo. These results were further validated in vivo, in a transplantation assay.

4 Discussion

In this work I sought to analyse the effects of Pcdh18a on cell dynamics and its possible role in axis elongation of zebrafish embryos.

4.1 Morphogenetic movements shape the embryo

The development of a complex organism from a single cell has long been one of the most fascinating phenomena in science. The incredible diversity of body structure and organization is elaborated early in animal development. During gastrulation, a series of well-coordinated events determine the embryonic axes, specify the primary germ layers and essentially shape the highly organized embryonic body. The essence of gastrulation is the coordinated migration of mesendodermal progenitor cells within the embryo. In general, gastrulation movements are achieved by a combination of motile cell behaviors. What are the essential cues to guide cell migration and how is this information displayed to cells are still not well understood and the correct positioning of cells along the body axis can be accomplished in different ways.

Different species can exploit different developmental strategies and use a variety of genetic programs in order to shape the embryonic axis. In mouse, the axial mesoderm is formed by three distinct cell populations of notochord progenitors, each displaying different morphogenetic processes; the anterior notochord progenitors directly converge on the midline, the trunk progenitors undergo medio-lateral intercalation and the most posterior cells actively migrate (Yamanaka et al., 2007). In chick, body axis elongation is accompanied by the posterior regression of the Hensen's node, the equivalent of the embryonic organizer (Spratt, 1947). On the contrary, in Xenopus, the elongation of the embryonic axis is entirely triggered by the medio-lateral intercalation of mesendoderm progenitors (Shih and Keller, 1992). Here the cells become polarized along their medio-lateral axis; they extend protrusions and converge towards the embryonic midline. Previous studies postulated that epiboly could be one of the driving forces of embryonic axis extension in zebrafish (Glickman et al., 2003). It has been further suggested that forces exerted by cells in the lateral plate mesoderm lead to the proper alignment of notochord progenitors (Tada and Heisenberg, 2012).

Based on my results, I propose that the posterior prechordal plate drives the extension of the zebrafish axis. In this thesis, I studied a distinct cell population in the anterior

midline of early zebrafish embryos that contributes to the proper elongation and organization of the notochord progenitors. Although, cells anteriorly located from the notochord progenitors have been known to exhibit active migration towards the animal pole in zebrafish, they have not been shown to play a role in axis elongation per se. My studies are the first to implicate that the anteriorly located Notochord Tip Cells can organize the trailing of the notochord progenitors.

My experiments showed that altered levels of Pcdh18a lead to severe developmental defects indicating that Pcdh18a has the capacity to interfere with morphogenetic processes (Figure 13, Figure 14). This has been a puzzling observation as such that Pcdh18a did not show any expression in the chordamesoderm. How could then a cell-cell adhesion protein have such a strong impact on axis formation?

4.2 How does Pcdh18a perturb axis formation?

Morphogenetic movements largely depend on the cell's ability to recognize its neighbours and the environmental cues. In this context, cell-cell connections have essential functions. During convergent extension in vertebrates, cells make connections via polarized cell protrusions and thus rearrange their cytoskeleton (Green and Davidson, 2007). These events have been shown to generate cellular tractions required for medio-lateral intercalation in Xenopus (Elul and Keller, 2000) (Wallingford et al., 2002). Even though, the generation of these traction forces does not require strong adhesion, the transient attachment of the leading edge of the cell to the substratum is essential for tail retraction (Webb et al., 2002).

Pcdhs have been implicated in sorting out of mesodermal cells by inducing cell shape changes (Kim et al, 1998, Yamamoto et al, 1998). Therefore it seemed plausible that Pcdh18a operates via a similar mechanism. I observed that notochord progenitor cells change their shape in the absence of Pcdh18a, they exhibit a more roundish profile and they did not reach the midline. This further indicates an indirect effect of Pcdh18 on the behavior of notochord progenitors. It seemed the most plausible explanation that Pcdh18a affects cell shape changes and cell behavior of posterior cells, thus most likely influencing the migratory properties of the cells. As member of the cadherin family, I found its expression in the cell membrane, in a punctate manner (Figure 17). By the end of gastrulation, Pcdh18a overexpressed in zebrafish embryos showed a subcellular localization at the posterior cell surface (Figure 25). Previous data suggest

that δ2-protocadherins can indeed accumulate at cell-cell contact sites (Hayashi and Takeichi, 2015).

I hypothesize that this connection is essential to pull the notochord progenitors towards the animal pole. In Xenopus, intercalation of cells in the lateral mesoderm could lead to the elongation of the axis. To test in a MO independent manner whether the anterior cell population has an essential function to the notochord progenitors, I ablated cell rows between the notochord progenitors and the NTCs.

If a similar case to Xenopus exists in zebrafish embryos, then the ablation experiments would not affect the migration of notochord progenitors. However, the opposite was true, ablated connection perturbed axial mesoderm formation and led to a short and broad axis (Figure 16). These results clearly establish that connection to the NTCs is essential and that the notochord progenitors most likely exhibit passive migration and act as followers during the active migration of the prechordal plate. It has been indeed shown that the extension rate of the notochord is greater than that of the lateral plate mesoderm (Glickman et al., 2003). This is in concordance with previous observations where ablation of neighbouring tissue affects notochord cells (Munro and Odell, 2002) suggesting that interaction with neighboring tissues is essential to the intercalation of notochord cells.

Taken together, my observation suggests a faster elongation rate compared to neighboring tissues and Pcdh18a could provide the driving force. This idea is also supported by the induced cell shape changes in the notochord and more evident from the ablation experiments: a connection between the NTCs and the following notochord progenitors is essential for axis elongation.

Although I used two different knockdown approaches to further examine the effects of Pcdh18a on the alignment of notochord cells, it would be an interesting idea to test what happens to notochord progenitors when the entire NTC population is ablated. The ablation of entire cell population could better address the function of a cell group instead of the knockdown of a particular protein. This could also determine the importance of Pcdh18a and the effects of the entire population on the notochord.

4.3 Pcdh18a interacts with E-cad

It is known that traction forces are transmitted via cell-cell adhesion molecules and exerted on the cytoskeleton. Many members of the cadherin family are directly

associated with actin filaments (Hayashi et al., 2014), although Pcdh18a is not directly associated with the cytoskeleton. The most obvious explanation is that as a cell adhesion molecule it could affect cell movements and alter migratory behavior. Therefore, a plausible explanation is that the effect of Pcdh18a on morphogenetic movements is indirect and exerted via other members of the cadherin superfamily. Classical cadherins have been indeed shown to be interacting partners of protocadherins. My co-localization studies further revealed a possible interaction between Pcdh18a and E-cad. However, my efforts to identify a physical interaction between these proteins by co-immunoprecipitation were not successful (data not shown). This could be due to the fact that E-cad and Pcdh18a localization was mainly observed in small endocytic vesicles that constitute only a portion of the entire E-cad pool in the cells. Therefore, the high background - coming from E-cad proteins not binding Pcdh18a - hinders the visualization of this interaction. The questions still remains what are the implications of the co-localization of E-cad and Pcdh18a?

The regulation of migratory behavior during gastrulation primarily depends on cell adhesiveness. Changes affecting adhesiveness can occur by different mechanisms such as transcriptional regulation and endocytotic trafficking of adhesion molecules.

Based on the observed distribution of E-cad in the presence of Pcdh18a and a shift to the recycling endysomes, I propose that Pcdh18a impacts the migratory behavior of cells by remodeling cell-cell adhesion at the cell membrane. Protocadherins have been shown to interact with other members of the classical cadherins and mediate their function. Pcdh19 controls cell movements during anterior neurulation via interaction with N-cad in zebrafish (Biswas et al, 2010). PAPC controls morphogenetic events by down-regulating the adhesive activity of the classical cadherin C-cadherin; a process, which is essential for normal gastrulation in the frog (Chen and Gumbiner, 2006). Furthermore, in cultured hippocampal neurons, induction of Pcdh8 results in binding of Pcdh8 to N-cad and to the subsequent internalization of the complex (Yasuda et al., 2007).

Pcdh18a also seems to play a role in E-cad trafficking. Upon enhancing Pcdh18a levels in zebrafish cells, E-cad specifically localized to the membrane and to Rab5 and Rab7 recycling endosomes (Figure 19). This implies that increased Pcdh18a levels could lead to the remodeling of E-cad in the NTCs during zebrafish development. If it is in fact the case, then it would allow the formation of a so-called adhesive gradient within the embryo that is essential for cell behavior

(Hammerschmidt and Wedlich, 2008). These quantitative differences are indeed required for the migration and sorting out of cells during gastrulation (Poole and Steinberg, 1982).

In a wound-healing assay, I could actually show that Pcdh18a affects migratory capabilities of cells, but only in the presence of E-cad (Figure 23). Cells only expressing Pcdh18 did not show any significant alteration in the migration speed. Upon blocking endocytosis, migration of E-cad positive cells was impaired; the reduced speed could be however rescued to a certain extent by adding Pcdh18a. Could this be the mechanism of action of Pcdh18a in the zebrafish prechordal plate?

During convergence and collective migration, cell connections are dynamically remodeled for cell migration but they still maintain adhesion within the migrating group. My results indicate that dynamic remodeling of E-cadherin-mediated adhesion takes place in the posterior prechordal plate. Pcdh18a is able to lead to the endocytosis of E-cadherin into Rab5 and Rab11 recycling endosomes.

Interestingly, a Pcdh18a mutant lacking the cytoplasmic domain (Pcdh18aΔICD) negatively influences E-cad endoyctosis suggesting that the intracellular domain of Pcdh18a is essential for the interaction with E-cad. (Figure 22). Several studies indeed suggest that regions in the cytoplasmic domain of δ2-protocadherins bear adhesion-suppressing functions reviewed in (Hayashi and Takeichi, 2015). Pcdh17 mutants lacking the cytoplasmic region stimulate lateral clumping of axons in the embryonic brain (Hayashi et al., 2014). Pcdh19 mutants lacking the cytoplasmic domain promote cell aggregation in L cells, a fibroblastic cell line (Tai et al., 2010). Thus, cytoplasmic regions of δ2-protocadherins appear to have an adhesion-inhibiting role.

4.4 Modeling of Pcdh18a effects on cell behavior

Results obtained from in situ hybridizations showed that an overlapping expression domain for Pcdh18a and E-cad, indicative of their presence in the same cell population. However, the molecular machinery that characterizes a mobile cell population such as the NTCs is a highly complex and organized system and examining every aspect of cell behavior in a simple set up *in vivo* has been challenging task.

Computational modeling, specifically the Cellular Potts Model has been widely used to model cellular mechanism and illuminate molecular mechanisms of collective cell

migration. In such a model, we showed that strong adhesion provided by E-cad and high cell motility provided by Pcdh18a-mediated remodeling of E-cad at the cell surface are indeed essential processes in gastrulating embryos. Interestingly, when NTCs did not exhibit high adhesiveness, the shape of the prechordal plate was rather perpendicular to the embryonic axis. This is in concordance with previous experimental data showing that E-cad loss and thus loss of cell adhesion in the prechordal plate perturbs active and directed migration of cells, and thereby also influences the trailing notochord progenitors (Heisenberg et al., 2000). On the other hand, high adhesiveness of NTCs similarly affected prechordal plate cells and notochord progenitors. Therefore, it is essential to keep a well-balance environment within the NTCs, which is achieved by trafficking of E-cad in a Pcdh18a-dependent manner.

Furthermore, I excluded the possibility that Pcdh18a regulates E-cad on the transcriptional level. Transciptomics analysis revealed that knockdown and overexpression of Pcdh18a did not lead to significant changes in the endogenous expression levels of E-cad. It is in concordance with previous observations that protocadherins do not generally regulate gene expression.

Interestingly, a recent studied showed that the axial protocadherin (AXPC) in Xenopus can affect notochordal morphogenesis, through its ability to regulate gene expression in the dorsal mesoderm and thus changes cell fate specification (Yoder and Gumbiner, 2011). As the transcriptomic analysis was based on the global alterations of Pcdh18a levels, a main concern was that it did not accurately reflect the in vivo situation. I indeed observed that Pcdh18a containing cells transplanted in the zebrafish embryos migrated in an organized fashion towards the animal pole and this organization resembled a rod-shape structure such as the notochord. However, in situ hybridizations proved that Pcdh18a indeed did not affect fate specification and expression levels of organizer genes in these embryos. Therefore it further strengthens the theory that the increase seen in the E-cad levels at the membrane could solely be the results of E-cad remodeling at the surface rather than the transcriptional regulation of the gene.

4.5 PCP signaling leads the way?

Cadherin activity and regulation has been also linked to components of the PCP pathway during vertebrate gastrulation (reviewed (Halbleib and Nelson, 2006). Zebrafish embryos, in which PCP signaling has been disrupted, exhibit a broadened notochord primordium and a subsequent defect in tail notochord development (Hammerschmidt et al., 1996). I observed a similar phenotype in embryos lacking Pcdh18a, indicating that PCP might be at play as the master regulator of gastrulation movements, in combination with Pcdh18a.

My observations suggested that E-cad might be stabilized in the membrane in a Pcdh18a-dependent manner, while Pcdh18a simultaneously enhanced E-cad localization to endosomes. In zebrafish, E-cad endocytosis is also triggered by the non-canonical PCP ligand Wnt11 (Ulrich et al., 2005) and localizes to Rab5c early recycling endosomes in the mesoderm. Interestingly, Pcdh18a also co-localizes with non-canonical PCP component such as Fzd7a in endocytic vesicles. In a wound-healing assay, Fzd7a was able to speed up cells, which is enhanced even more in the presence of Pcdh18a indicating that the presence of both Fzd7a and Pcdh18a positively influenced E-cad recycling. It is therefore a possible explanation that the effects of PCP signaling and Pcdh18a converge on the same level: the endocytic trafficking of E-cad. Previously published data demonstrated that PAPC suppresses C-cadherin-mediated cell adhesion and promotes the Wnt-PCP pathway-dependent cell motility (Chen and Gumbiner, 2006). Nevertheless, further experiments will decide whether PCP signaling can directly affect Pcdh18a or these two mechanisms act independently from each other in gastrulation.

4.6 Conclusions

My experiments suggest a revised model of morphogenetic movements and their regulation in zebrafish gastrulation. E-cad is most strongly expressed in the zebrafish prechordal plate and affects its active migration towards the animal pole (Tada, 2012 and Figure 7). In the region of NTCs, Pcdh18a influences the presentation of E-cad at the membrane by endocytic trafficking (Figure 19). This mechanism could lead to changes in adhesiveness and migratory behavior of NTCs relative to neighboring tissues. NTCs could thus determine the direction of cell movements. Furthermore, we

speculate that adhesion gradients could affect sorting out of NTCs from notochord progenitors (Pcdh18a positive and negative cells sort out, (Aamar and Dawid, 2008)) thereby reinforcing the shaping of the notochord.

Based on my results, I propose an extended model for cell migration movements and axial mesoderm organization during gastrulation (Figure 30).

At the onset of gastrulation, progenitors of the prechordal plate start to internalize and form a tightly connected cell group whose migration is directed by E-cad and Wnt/PCP signaling. The posterior prechordal plate constitutes the notochord tip cells, the NTCs; a cohesive group that is held together by the strong cell-cell adhesion mediated by E-cadherin. However, the remodeling of the E-cad presentation in the membrane and thus determining cell adhesiveness allows NTCs to acquire fast migratory properties. NTCs march towards the animal pole and push the anteriorly located mesodermal cells in front of them, leading to the formation of a convexly curved prechordal plate.

In the posterior axial mesoderm, NTC - migration results in the correct positioning of notochord progenitors along the midline. NTCs simultaneously exert pulling forces on the notochord progenitors and does so by Pcdh18a mediated connections at the posterior cell surface.

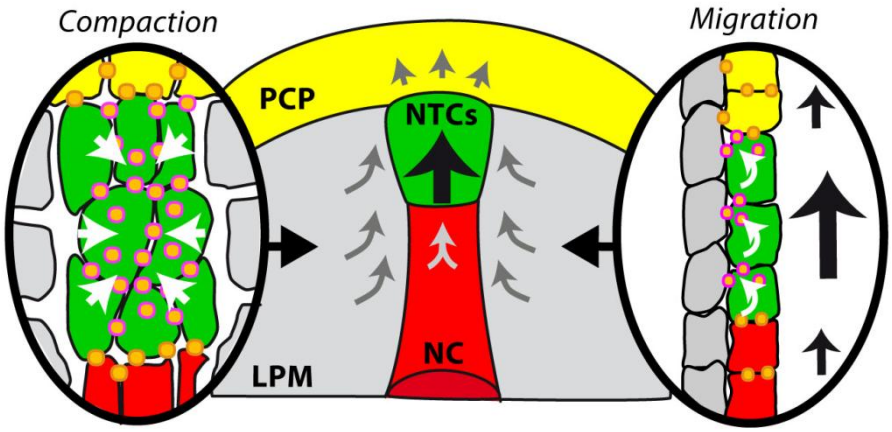

Figure 30 Schematic summary of the proposed function of the NTCs in notochord formation.

Pcdh18a/E-cadherin adhesion complexes (orange/pink dots) increase cell adhesion within the NTCs, leading to their compact organization (left). In parallel, Pcdh18a controls recycling of E-cadherin to allow fast cohort migration of the NTCs (right), most likely leading to simultaneous "pushing" forces on the anterior prechordal plate and "pulling" forces on the notochord progenitors.

PCP –prechordal plate, NTC – notochord tip cells, NC – notochord, LPM – lateral plate mesoderm

4.7 Outlook

Although the experimental data obtained in this thesis brings us closer to the understanding of the complexity of embryogenesis in zebrafish there are still interesting questions that needs to be answered. As seen from the simulation, high motility and adhesiveness are prerequisite for the elongation of the embryonic axis. It would be interesting to test on the single cell level whether Pcdh18a can indeed lead to different net imbalance in traction forces.

It is also important to analyse whether Pcdh18a could operate in cell migration via indirect interactions to the cytoskeleton. In fact, δ-protocadherins members have been shown to interact with actin filament and thereby modulate cell migration (Takeichi et al, 2014). This could be a possible mechanism for Pcdh18a since I observed its expression on cell protrusion. Further characterization of these protrusions and testing whether Pcdh18a co-localizes with the WAVE complex could bring us forward in elucidating its mechanism on axis elongation. This additional knowledge could further highlight aspects of Pcdh18a function in cell migration and on global levels in the zebrafish embryo.

5 Appendix

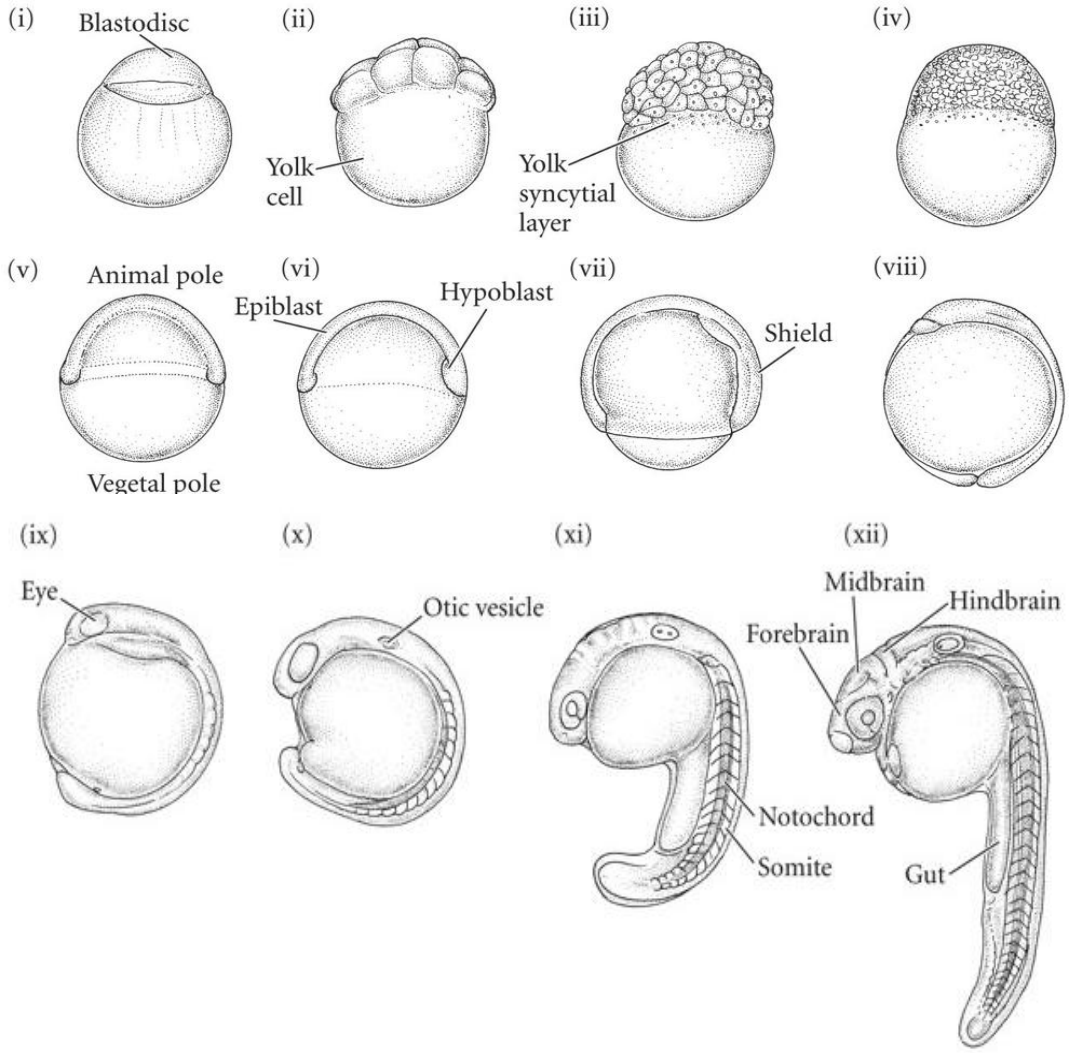

Figure 31 Rapid development of zebrafish.

Shorty after fertilization, the cytoplasm (blastodisc) separates from the yolk cells (i, ii). Synchronized division of the blastodisc starts and generates a mound of cells, the blastoderm (iii,iv). Cell movements start at blastula stage, by the process of epiboly, the blastoderm start to thin and spread over the yolk. By 50% epiboly, half of the yolk cell is covered (v). During gastrulation (vi-viii), cells starts to move inward, forming the outer layer of epiblast and the prospective mesoderm progenitors, the hypoblast (vi). At the stage of shield formation, the embryonic organizer is visible and defines the future dorsal side of the embryo (vi). Cells accumulate in the midline and move towards the animal pole (vii). By the end of gastrulation, the blastoderm entirely engulfs the yolk cell and the tailbud becomes visible (viii).
In the next stages of somitogenesis (ix-xii), the rudiments of the primary organs appear; the eye starts to form and otic vesicle is apparent. By 20 hours after fertilization (xi), the notochord and somites can

be separated. At 24 hpf, at the beginning of the pharyngula stage, all major compartments of the brain are formed (xii). Adapted from Gilbert, 2008, originally described by Kimmel et al, 1995

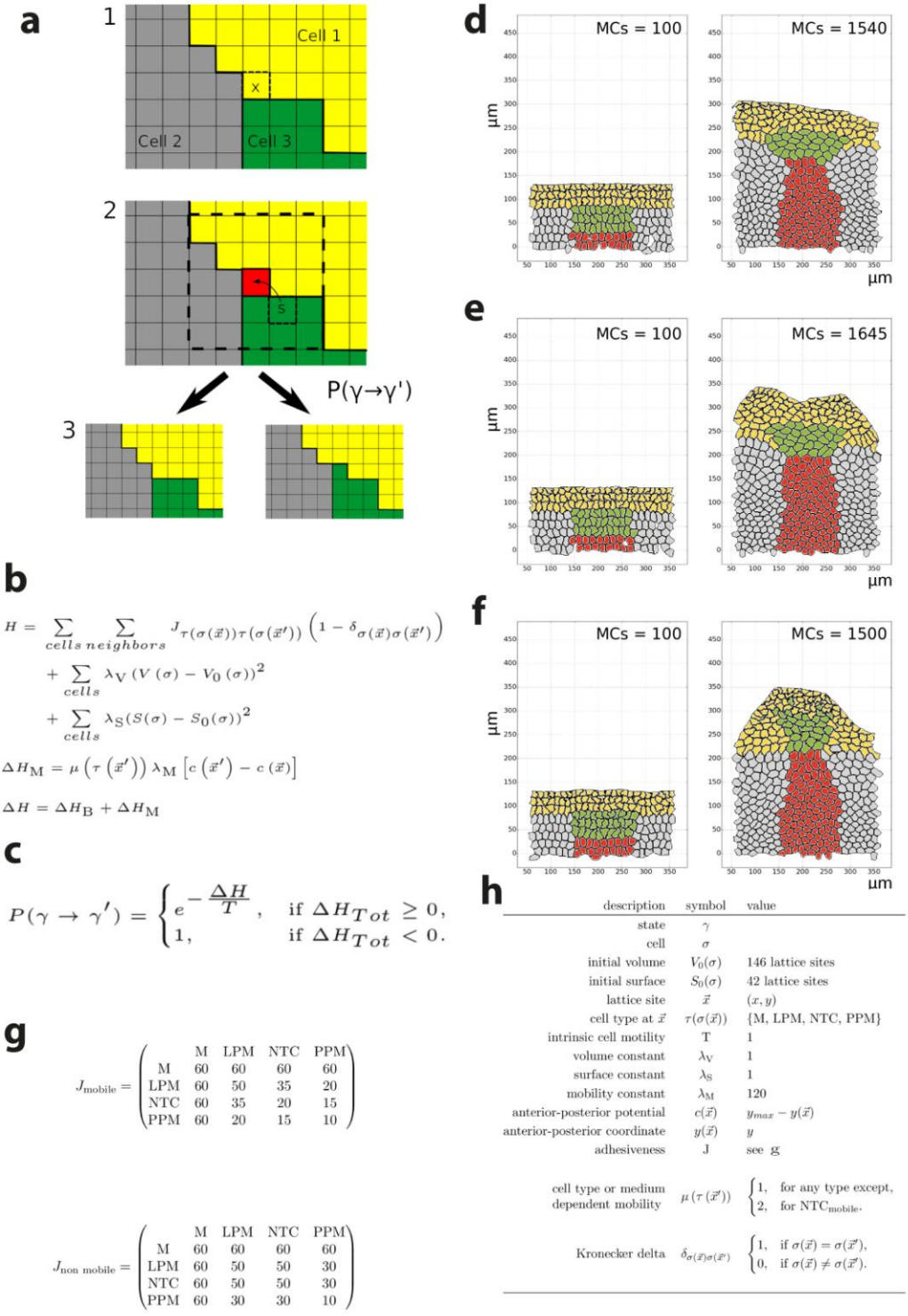

Figure 32 Simulation parameters and equations

References

AAMAR, E. & DAWID, I. B. 2008. Protocadherin-18a has a role in cell adhesion, behavior and migration in zebrafish development. *Dev Biol,* 318**,** 335-46.

ADLER, P. N. 2002. Planar signaling and morphogenesis in Drosophila. *Dev Cell,* 2**,** 525-35.

AOKI, E., KIMURA, R., SUZUKI, S. T. & HIRANO, S. 2003. Distribution of OL-protocadherin protein in correlation with specific neural compartments and local circuits in the postnatal mouse brain. *Neuroscience,* 117**,** 593-614.

BAKI, L., MARAMBAUD, P., EFTHIMIOPOULOS, S., GEORGAKOPOULOS, A., WEN, P., CUI, W., SHIOI, J., KOO, E., OZAWA, M., FRIEDRICH, V. L., JR. & ROBAKIS, N. K. 2001. Presenilin-1 binds cytoplasmic epithelial cadherin, inhibits cadherin/p120 association, and regulates stability and function of the cadherin/catenin adhesion complex. *Proc Natl Acad Sci U S A,* 98**,** 2381-6.

BAKKERS, J., KRAMER, C., POTHOF, J., QUAEDVLIEG, N. E., SPAINK, H. P. & HAMMERSCHMIDT, M. 2004. Has2 is required upstream of Rac1 to govern dorsal migration of lateral cells during zebrafish gastrulation. *Development,* 131**,** 525-37.

BROCKERHOFF, S. E., HURLEY, J. B., JANSSEN-BIENHOLD, U., NEUHAUSS, S. C., DRIEVER, W. & DOWLING, J. E. 1995. A behavioral screen for isolating zebrafish mutants with visual system defects. *Proc Natl Acad Sci U S A,* 92**,** 10545-9.

CAMPBELL, K. & CASANOVA, J. 2015. A role for E-cadherin in ensuring cohesive migration of a heterogeneous population of non-epithelial cells. *Nat Commun,* 6**,** 7998.

CARMANY-RAMPEY, A. & SCHIER, A. F. 2001. Single-cell internalization during zebrafish gastrulation. *Curr Biol,* 11**,** 1261-5.

CAVALLARO, U. & DEJANA, E. 2011. Adhesion molecule signalling: not always a sticky business. *Nat Rev Mol Cell Biol,* 12**,** 189-97.

CHAVRIER, P., PARTON, R. G., HAURI, H. P., SIMONS, K. & ZERIAL, M. 1990. Localization of low molecular weight GTP binding proteins to exocytic and endocytic compartments. *Cell,* 62**,** 317-29.

CHEN, X. & GUMBINER, B. M. 2006. Paraxial protocadherin mediates cell sorting and tissue morphogenesis by regulating C-cadherin adhesion activity. *J Cell Biol,* 174**,** 301-13.

CLARK, B. S., WINTER, M., COHEN, A. R. & LINK, B. A. 2011. Generation of Rab-based transgenic lines for in vivo studies of endosome biology in zebrafish. *Dev Dyn,* 240**,** 2452-65.

COOK, N. R., ROW, P. E. & DAVIDSON, H. W. 2004. Lysosome associated membrane protein 1 (Lamp1) traffics directly from the TGN to early endosomes. *Traffic,* 5**,** 685-99.

CROSNIER, C., STAMATAKI, D. & LEWIS, J. 2006. Organizing cell renewal in the intestine: stem cells, signals and combinatorial control. *Nat Rev Genet,* 7**,** 349-59.

DEVENPORT, D. 2014. The cell biology of planar cell polarity. *J Cell Biol,* 207**,** 171-9.

DUGUAY, D., FOTY, R. A. & STEINBERG, M. S. 2003. Cadherin-mediated cell adhesion and tissue segregation: qualitative and quantitative determinants. *Dev Biol,* 253**,** 309-23.

DUMORTIER, J. G., MARTIN, S., MEYER, D., ROSA, F. M. & DAVID, N. B. 2012. Collective mesendoderm migration relies on an intrinsic directionality signal transmitted through cell contacts. *Proc Natl Acad Sci U S A,* 109**,** 16945-50.

ELUL, T. & KELLER, R. 2000. Monopolar protrusive activity: a new morphogenic cell behavior in the neural plate dependent on vertical interactions with the mesoderm in Xenopus. *Dev Biol,* 224**,** 3-19.

FELDMAN, B., CONCHA, M. L., SAUDE, L., PARSONS, M. J., ADAMS, R. J., WILSON, S. W. & STEMPLE, D. L. 2002. Lefty antagonism of Squint is essential for normal gastrulation. *Curr Biol,* 12**,** 2129-35.

FRIEDL, P. & GILMOUR, D. 2009. Collective cell migration in morphogenesis, regeneration and cancer. *Nat Rev Mol Cell Biol,* 10**,** 445-57.

FUJITA, Y., KRAUSE, G., SCHEFFNER, M., ZECHNER, D., LEDDY, H. E., BEHRENS, J., SOMMER, T. & BIRCHMEIER, W. 2002. Hakai, a c-Cbl-like protein, ubiquitinates and induces endocytosis of the E-cadherin complex. *Nat Cell Biol,* 4**,** 222-31.

GLICKMAN, N. S., KIMMEL, C. B., JONES, M. A. & ADAMS, R. J. 2003. Shaping the zebrafish notochord. *Development,* 130**,** 873-87.

GRANER, F. & GLAZIER, J. A. 1992. Simulation of biological cell sorting using a two-dimensional extended Potts model. *Phys Rev Lett,* 69**,** 2013-2016.

GRAY, R. S., ROSZKO, I. & SOLNICA-KREZEL, L. 2011. Planar cell polarity: coordinating morphogenetic cell behaviors with embryonic polarity. *Dev Cell,* 21**,** 120-33.

GREEN, J. B. & DAVIDSON, L. A. 2007. Convergent extension and the hexahedral cell. *Nat Cell Biol,* 9**,** 1010-5.

HALBLEIB, J. M. & NELSON, W. J. 2006. Cadherins in development: cell adhesion, sorting, and tissue morphogenesis. *Genes Dev,* 20**,** 3199-214.

HAMMERSCHMIDT, M., PELEGRI, F., MULLINS, M. C., KANE, D. A., BRAND, M., VAN EEDEN, F. J., FURUTANI-SEIKI, M., GRANATO, M., HAFFTER, P., HEISENBERG, C. P., JIANG, Y. J., KELSH, R. N., ODENTHAL, J., WARGA, R. M. & NUSSLEIN-VOLHARD, C. 1996. Mutations affecting morphogenesis during gastrulation and tail formation in the zebrafish, Danio rerio. *Development,* 123**,** 143-51.

HAMMERSCHMIDT, M. & WEDLICH, D. 2008. Regulated adhesion as a driving force of gastrulation movements. *Development,* 135**,** 3625-41.

HAYASHI, S., INOUE, Y., KIYONARI, H., ABE, T., MISAKI, K., MORIGUCHI, H., TANAKA, Y. & TAKEICHI, M. 2014. Protocadherin-17 mediates collective axon extension by recruiting actin regulator complexes to interaxonal contacts. *Dev Cell,* 30**,** 673-87.

HAYASHI, S. & TAKEICHI, M. 2015. Emerging roles of protocadherins: from self-avoidance to enhancement of motility. *J Cell Sci,* 128**,** 1455-64.

HAZAN, R. B., QIAO, R., KEREN, R., BADANO, I. & SUYAMA, K. 2004. Cadherin switch in tumor progression. *Ann N Y Acad Sci,* 1014**,** 155-63.

HEISENBERG, C. P., TADA, M., RAUCH, G. J., SAUDE, L., CONCHA, M. L., GEISLER, R., STEMPLE, D. L., SMITH, J. C. & WILSON, S. W. 2000. Silberblick/Wnt11 mediates convergent extension movements during zebrafish gastrulation. *Nature,* 405**,** 76-81.

HIRANO, S., SUZUKI, S. T. & REDIES, C. 2003. The cadherin superfamily in neural development: diversity, function and interaction with other molecules. *Front Biosci,* 8**,** d306-55.

HIRANO, S., YAN, Q. & SUZUKI, S. T. 1999. Expression of a novel protocadherin, OL-protocadherin, in a subset of functional systems of the developing mouse brain. *J Neurosci,* 19**,** 995-1005.

HOMAYOUNI, R., RICE, D. S. & CURRAN, T. 2001. Disabled-1 interacts with a novel developmentally regulated protocadherin. *Biochem Biophys Res Commun,* 289**,** 539-47.

HONG, E. & BREWSTER, R. 2006. N-cadherin is required for the polarized cell behaviors that drive neurulation in the zebrafish. *Development,* 133**,** 3895-905.

HOWELL, B. W., HERRICK, T. M., HILDEBRAND, J. D., ZHANG, Y. & COOPER, J. A. 2000. Dab1 tyrosine phosphorylation sites relay positional signals during mouse brain development. *Curr Biol,* 10**,** 877-85.

HWANG, W. Y., FU, Y., REYON, D., MAEDER, M. L., TSAI, S. Q., SANDER, J. D., PETERSON, R. T., YEH, J. R. & JOUNG, J. K. 2013. Efficient genome editing in zebrafish using a CRISPR-Cas system. *Nat Biotechnol,* 31**,** 227-9.

JENKINS, P. M., VASAVDA, C., HOSTETTLER, J., DAVIS, J. Q., ABDI, K. & BENNETT, V. 2013. E-cadherin polarity is determined by a multifunction motif mediating lateral membrane retention through ankyrin-G and apical-lateral transcytosis through clathrin. *J Biol Chem,* 288**,** 14018-31.

JOWETT, T. & LETTICE, L. 1994. Whole-mount in situ hybridizations on zebrafish embryos using a mixture of digoxigenin- and fluorescein-labelled probes. *Trends Genet,* 10**,** 73-4.

KASNAUSKIENE, J., CIULADAITE, Z., PREIKSAITIENE, E., MATULEVICIENE, A., ALEXANDROU, A., KOUMBARIS, G., SISMANI, C., PEPALYTE, I., PATSALIS, P. C. & KUCINSKAS, V. 2012. A single gene deletion on 4q28.3: PCDH18--a new candidate gene for intellectual disability? *Eur J Med Genet,* 55**,** 274-7.

KELLER, R. 1991. Early embryonic development of Xenopus laevis. *Methods Cell Biol,* 36**,** 61-113.

KELLER, R. E. 1980. The cellular basis of epiboly: an SEM study of deep-cell rearrangement during gastrulation in Xenopus laevis. *J Embryol Exp Morphol,* 60**,** 201-34.

KELLER, R. E., DANILCHIK, M., GIMLICH, R. & SHIH, J. 1985. The function and mechanism of convergent extension during gastrulation of Xenopus laevis. *J Embryol Exp Morphol,* 89 Suppl**,** 185-209.

KIM, S. H., YAMAMOTO, A., BOUWMEESTER, T., AGIUS, E. & ROBERTIS, E. M. 1998. The role of paraxial protocadherin in selective adhesion and cell movements of the mesoderm during Xenopus gastrulation. *Development,* 125**,** 4681-90.

KIMMEL, C. B., BALLARD, W. W., KIMMEL, S. R., ULLMANN, B. & SCHILLING, T. F. 1995. Stages of embryonic development of the zebrafish. *Dev Dyn,* 203**,** 253-310.

KIMMEL, C. B., WARGA, R. M. & SCHILLING, T. F. 1990. Origin and organization of the zebrafish fate map. *Development,* 108**,** 581-94.

MAYOR, R. & ETIENNE-MANNEVILLE, S. 2016. The front and rear of collective cell migration. *Nat Rev Mol Cell Biol,* 17**,** 97-109.

MLODZIK, M. 1999. Planar polarity in the Drosophila eye: a multifaceted view of signaling specificity and cross-talk. *EMBO J,* 18**,** 6873-9.

MONTERO, J. A., CARVALHO, L., WILSCH-BRAUNINGER, M., KILIAN, B., MUSTAFA, C. & HEISENBERG, C. P. 2005. Shield formation at the onset of zebrafish gastrulation. *Development,* 132**,** 1187-98.

MUNRO, E. M. & ODELL, G. 2002. Morphogenetic pattern formation during ascidian notochord formation is regulative and highly robust. *Development,* 129**,** 1-12.

MURATA, Y., HAMADA, S., MORISHITA, H., MUTOH, T. & YAGI, T. 2004. Interaction with protocadherin-gamma regulates the cell surface expression of protocadherin-alpha. *J Biol Chem,* 279**,** 49508-16.

MYERS, D. C., SEPICH, D. S. & SOLNICA-KREZEL, L. 2002. Bmp activity gradient regulates convergent extension during zebrafish gastrulation. *Dev Biol,* 243**,** 81-98.

NASEVICIUS, A. & EKKER, S. C. 2000. Effective targeted gene 'knockdown' in zebrafish. *Nat Genet,* 26**,** 216-20.

NIEHRS, C. 2012. The complex world of WNT receptor signalling. *Nat Rev Mol Cell Biol,* 13**,** 767-79.

NIETO, M. A. 2011. The ins and outs of the epithelial to mesenchymal transition in health and disease. *Annu Rev Cell Dev Biol,* 27**,** 347-76.

PAUL, R., EWING, C. M., JARRARD, D. F. & ISAACS, W. B. 1997. The cadherin cell-cell adhesion pathway in prostate cancer progression. *Br J Urol,* 79 Suppl 1**,** 37-43.

PEREZ, T. D. & NELSON, W. J. 2004. Cadherin adhesion: mechanisms and molecular interactions. *Handb Exp Pharmacol*, 3-21.

POOLE, T. J. & STEINBERG, M. S. 1982. Evidence for the guidance of pronephric duct migration by a craniocaudally traveling adhesion gradient. *Dev Biol,* 92**,** 144-58.

REICHMAN-FRIED, M., MININA, S. & RAZ, E. 2004. Autonomous modes of behavior in primordial germ cell migration. *Dev Cell,* 6**,** 589-96.

ROBERTS, R. L., BARBIERI, M. A., ULLRICH, J. & STAHL, P. D. 2000. Dynamics of rab5 activation in endocytosis and phagocytosis. *J Leukoc Biol,* 68**,** 627-32.

ROHDE, L. A. & HEISENBERG, C. P. 2007. Zebrafish gastrulation: cell movements, signals, and mechanisms. *Int Rev Cytol,* 261**,** 159-92.

SANO, K., TANIHARA, H., HEIMARK, R. L., OBATA, S., DAVIDSON, M., ST JOHN, T., TAKETANI, S. & SUZUKI, S. 1993. Protocadherins: a large family of cadherin-related molecules in central nervous system. *EMBO J,* 12**,** 2249-56.

SCARPA, E. & MAYOR, R. 2016. Collective cell migration in development. *J Cell Biol,* 212**,** 143-55.

SCHREINER, D. & WEINER, J. A. 2010. Combinatorial homophilic interaction between gamma-protocadherin multimers greatly expands the molecular diversity of cell adhesion. *Proc Natl Acad Sci U S A,* 107**,** 14893-8.

SCHULTE-MERKER, S., VAN EEDEN, F. J., HALPERN, M. E., KIMMEL, C. B. & NUSSLEIN-VOLHARD, C. 1994. no tail (ntl) is the zebrafish homologue of the mouse T (Brachyury) gene. *Development,* 120**,** 1009-15.

SEIFERT, J. R. & MLODZIK, M. 2007. Frizzled/PCP signalling: a conserved mechanism regulating cell polarity and directed motility. *Nat Rev Genet,* 8**,** 126-38.

SEPICH, D. S., MYERS, D. C., SHORT, R., TOPCZEWSKI, J., MARLOW, F. & SOLNICA-KREZEL, L. 2000. Role of the zebrafish trilobite locus in gastrulation movements of convergence and extension. *Genesis,* 27**,** 159-73.

SHEN, M. M. 2007. Nodal signaling: developmental roles and regulation. *Development,* 134**,** 1023-34.

SHIH, J. & KELLER, R. 1992. Cell motility driving mediolateral intercalation in explants of Xenopus laevis. *Development,* 116**,** 901-14.

SHIMIZU, T., YABE, T., MURAOKA, O., YONEMURA, S., ARAMAKI, S., HATTA, K., BAE, Y. K., NOJIMA, H. & HIBI, M. 2005. E-cadherin is required for gastrulation cell movements in zebrafish. *Mech Dev,* 122**,** 747-63.

SIMON, A. R., VIKIS, H. G., STEWART, S., FANBURG, B. L., COCHRAN, B. H. & GUAN, K. L. 2000. Regulation of STAT3 by direct binding to the Rac1 GTPase. *Science,* 290**,** 144-7.

SOLNICA-KREZEL, L. 2006. Gastrulation in zebrafish -- all just about adhesion? *Curr Opin Genet Dev,* 16**,** 433-41.

SOLNICA-KREZEL, L. & COOPER, M. S. 2002. Cellular and genetic mechanisms of convergence and extension. *Results Probl Cell Differ,* 40**,** 136-65.

SOLNICA-KREZEL, L. & SEPICH, D. S. 2012. Gastrulation: making and shaping germ layers. *Annu Rev Cell Dev Biol,* 28**,** 687-717.

SOMSEL RODMAN, J. & WANDINGER-NESS, A. 2000. Rab GTPases coordinate endocytosis. *J Cell Sci,* 113 Pt 2**,** 183-92.

SPRATT, N. T., JR. 1947. Regression and shortening of the primitive streak in the explanted chick blastoderm. *J Exp Zool,* 104**,** 69-100.

STEINBERG, M. S. 2007. Differential adhesion in morphogenesis: a modern view. *Curr Opin Genet Dev,* 17**,** 281-6.

STRATHDEE, G. 2002. Epigenetic versus genetic alterations in the inactivation of E-cadherin. *Semin Cancer Biol,* 12**,** 373-9.

SYMES, K. & MERCOLA, M. 1996. Embryonic mesoderm cells spread in response to platelet-derived growth factor and signaling by phosphatidylinositol 3-kinase. *Proc Natl Acad Sci U S A,* 93**,** 9641-4.

TADA, M. & HEISENBERG, C. P. 2012. Convergent extension: using collective cell migration and cell intercalation to shape embryos. *Development,* 139**,** 3897-904.

TAI, K., KUBOTA, M., SHIONO, K., TOKUTSU, H. & SUZUKI, S. T. 2010. Adhesion properties and retinofugal expression of chicken protocadherin-19. *Brain Res,* 1344**,** 13-24.

TAKAHASHI, S., KUBO, K., WAGURI, S., YABASHI, A., SHIN, H. W., KATOH, Y. & NAKAYAMA, K. 2012. Rab11 regulates exocytosis of recycling vesicles at the plasma membrane. *J Cell Sci,* 125**,** 4049-57.

TAKEICHI, M. 1988. The cadherins: cell-cell adhesion molecules controlling animal morphogenesis. *Development,* 102**,** 639-55.

THIERY, J. P. 2002. Epithelial-mesenchymal transitions in tumour progression. *Nat Rev Cancer,* 2**,** 442-54.

TRINKAUS, J. P. 1992. The midblastula transition, the YSL transition and the onset of gastrulation in Fundulus. *Dev Suppl***,** 75-80.

ULRICH, F., CONCHA, M. L., HEID, P. J., VOSS, E., WITZEL, S., ROEHL, H., TADA, M., WILSON, S. W., ADAMS, R. J., SOLL, D. R. & HEISENBERG, C. P. 2003. Slb/Wnt11 controls hypoblast cell migration and morphogenesis at the onset of zebrafish gastrulation. *Development,* 130**,** 5375-84.

ULRICH, F. & HEISENBERG, C. P. 2008. Probing E-cadherin endocytosis by morpholino-mediated Rab5 knockdown in zebrafish. *Methods Mol Biol,* 440**,** 371-87.

ULRICH, F., KRIEG, M., SCHOTZ, E. M., LINK, V., CASTANON, I., SCHNABEL, V., TAUBENBERGER, A., MUELLER, D., PUECH, P. H. & HEISENBERG, C. P. 2005. Wnt11 functions in gastrulation by controlling cell cohesion through Rab5c and E-cadherin. *Dev Cell,* 9**,** 555-64.

VAZQUEZ-CINTRON, E. J., MONU, N. R., BURNS, J. C., BLUM, R., CHEN, G., LOPEZ, P., MA, J., RADOJA, S. & FREY, A. B. 2012. Protocadherin-18 is a novel differentiation marker and an inhibitory signaling receptor for CD8+ effector memory T cells. *PLoS One,* 7**,** e36101.

VEEMAN, M. T., AXELROD, J. D. & MOON, R. T. 2003. A second canon. Functions and mechanisms of beta-catenin-independent Wnt signaling. *Dev Cell,* 5**,** 367-77.

VON DER HARDT, S., BAKKERS, J., INBAL, A., CARVALHO, L., SOLNICA-KREZEL, L., HEISENBERG, C. P. & HAMMERSCHMIDT, M. 2007. The Bmp gradient of the zebrafish gastrula guides migrating lateral cells by regulating cell-cell adhesion. *Curr Biol,* 17**,** 475-87.

WALCK-SHANNON, E. & HARDIN, J. 2014. Cell intercalation from top to bottom. *Nat Rev Mol Cell Biol,* 15**,** 34-48.

WALLINGFORD, J. B., FRASER, S. E. & HARLAND, R. M. 2002. Convergent extension: the molecular control of polarized cell movement during embryonic development. *Dev Cell,* 2**,** 695-706.

WARGA, R. M. & KIMMEL, C. B. 1990. Cell movements during epiboly and gastrulation in zebrafish. *Development,* 108**,** 569-80.

WARGA, R. M. & NUSSLEIN-VOLHARD, C. 1998. spadetail-dependent cell compaction of the dorsal zebrafish blastula. *Dev Biol,* 203**,** 116-21.

WEBB, D. J., PARSONS, J. T. & HORWITZ, A. F. 2002. Adhesion assembly, disassembly and turnover in migrating cells -- over and over and over again. *Nat Cell Biol,* 4**,** E97-100.

WINKLBAUER, R., MEDINA, A., SWAIN, R. K. & STEINBEISSER, H. 2001. Frizzled-7 signalling controls tissue separation during Xenopus gastrulation. *Nature,* 413**,** 856-60.

YAMANAKA, Y., TAMPLIN, O. J., BECKERS, A., GOSSLER, A. & ROSSANT, J. 2007. Live imaging and genetic analysis of mouse notochord formation reveals regional morphogenetic mechanisms. *Dev Cell,* 13**,** 884-96.

YASUDA, S., TANAKA, H., SUGIURA, H., OKAMURA, K., SAKAGUCHI, T., TRAN, U., TAKEMIYA, T., MIZOGUCHI, A., YAGITA, Y., SAKURAI, T., DE ROBERTIS, E. M. & YAMAGATA, K. 2007. Activity-induced protocadherin arcadlin regulates dendritic spine number by triggering N-cadherin endocytosis via TAO2beta and p38 MAP kinases. *Neuron,* 56**,** 456-71.

YODER, M. D. & GUMBINER, B. M. 2011. Axial protocadherin (AXPC) regulates cell fate during notochordal morphogenesis. *Dev Dyn,* 240**,** 2495-504.

YOSHIDA, C. & TAKEICHI, M. 1982. Teratocarcinoma cell adhesion: identification of a cell-surface protein involved in calcium-dependent cell aggregation. *Cell,* 28**,** 217-24.

YOSHIDA, K., WATANABE, M., KATO, H., DUTTA, A. & SUGANO, S. 1999. BH-protocadherin-c, a member of the cadherin superfamily, interacts with protein phosphatase 1 alpha through its intracellular domain. *FEBS Lett,* 460**,** 93-8.

ZHU, X., XU, Y., YU, S., LU, L., DING, M., CHENG, J., SONG, G., GAO, X., YAO, L., FAN, D., MENG, S., ZHANG, X., HU, S. & TIAN, Y. 2014. An efficient genotyping method for genome-modified animals and human cells generated with CRISPR/Cas9 system. *Sci Rep,* 4**,** 6420.